



Technische Universität Wien Fakultät für Mathematik und Geoinformation Department für Geodäsie und Geoinformation

# **DIPLOMARBEIT**

Comparative Analysis of Airborne Laser Scanning and Image Matching Point Clouds in Forestry: Enhancing Temporal Resolution using Machine Learning

zur Erlangung des akademischen Grades

Diplom-Ingenieur (Dipl.-Ing.)

im Rahmen des Masterstudiums

Geodäsie und Geoinformation

eingereicht von

Lorenz Schimpl, BSc Matrikelnummer 11704951

ausgeführt am

Department für Geodäsie und Geoinformation der Fakultät für Mathematik und Geoinformation der Technischen Universität Wien

unter der Betreuung von:

Univ.Prof. Dipl.-Ing. Dr.techn. Norbert Pfeifer

unter der Mitwirkung von:

Anna Iglseder, BSc MSc

Dipl.-Ing. Dr.techn. Markus Hollaus

Wien, 01.12.2023 Unterschrift Verfasser Unterschrift Betreuer



# Eidesstattliche Erklärung

Ich erkläre an Eides statt, dass ich die vorliegende Arbeit selbstständig und nach den anerkannten Grundsätzen für wissenschaftliche Arbeiten verfasst habe. Alle verwendeten Quellen, insbesondere die zugrundeliegende Literatur, sind in dieser Arbeit genannt und angeführt. Die direkt aus den Quellen übernommenen Passagen sind als solche gekennzeichnet.

Das Thema dieser Arbeit wurde von mir weder in Osterreich noch im Ausland in irgendeiner Form als Prüfungsarbeit einem Gutachter zur Beurteilung vorgelegt.

Wien, am 01. Dezember 2023

Lorenz Schimpl



# **Danksagung**

Zuerst möchte ich mich bei meinen beiden BetreuerInnen, Anna Iglseder und Markus Hollaus, herzlich bedanken. Ich schätze nicht nur euer unglaubliches Wissen und eure Erfahrung, sondern auch die unzähligen Meetings, die mir bei der Erstellung dieser Arbeit geholfen haben. Vielen Dank auch für das Vertrauen und die Möglichkeit, in verschiedenen Projekten wertvolle Erfahrungen zu sammeln und neues Wissen zu erlangen.

Des Weiteren möchte ich mich auch gerne bei Herrn Prof. Pfeifer bedanken, dass er mir die Möglichkeit gegeben hat, in der Forschungsgruppe zu arbeiten und im Rahmen dieser Tätigkeit meine Kenntnisse in verschiedenen Bereichen zu vertiefen. Besonderer Dank gilt auch Sebastian Mikolka-Flöry, der mir immer in allen Belangen geholfen hat. Danke, dass du mir immer wieder gesagt hast, wie wichtig und praktisch es ist, programmieren zu lernen! Weiterer Dank gilt auch meinen KollegInnen der Photogrammetrie, besonders Johannes Otepka-Schremmer für die Beratung in allen OPALS-Angelegenheiten sowie Camillo Ressl und Gottfried Mandlburger, die mit ihrem großen Fachwissen immer beratend bei Fragen zu den Daten zur Stelle waren.

Bedanken möchte ich mich auch bei meinen beiden KommilitonInnen, Anne und Clemens. Danke für die unzähligen Stunden, die wir gemeinsam in Online-Meetings verbracht haben, und dafür, dass wir zusammen gelernt, gelacht und nun auch gearbeitet haben!

Großen Dank möchte ich vor allem an meine Eltern aussprechen, die es mir überhaupt erst ermöglicht haben, in Wien zu studieren und zu leben. Danke, dass ihr immer an mich geglaubt und mich unterstützt habt.

Zuletzt möchte ich mich bei Sandra bedanken. Danke, dass du immer für mich da bist und mich in allen Belangen unterstützt hast. Danke für dein Verständnis in stressigen Zeiten und für all unsere schönen gemeinsamen Erlebnisse!

# Kurzfassung

Luftgestützte Laserscanning-Punktwolken werden landesweit zur Erstellung digitaler Oberflächenmodelle und weiterführend zur Ableitung von Informationen über Waldgebiete verwendet. Diese Aufnahmemethode gilt bis dato als state-of-the-art bei der Aufnahme, vor allem in bewaldeten Gebieten. Da diese jedoch in Österreich und Europa zwar regelmäßig, jedoch selten erstellt werden, ist die Modellierung basierend auf Airborne-Laserscanning-Daten (ALS) von Waldparametern in hoher zeitlicher Auflösung schwierig. Insbesondere die Ableitung von dynamischen Informationen wie Biomasse oder der Zustand eines Baumbestandes nach Umweltereignissen wie Unwettern oder Waldbränden beziehungsweise das Monitoring von Schutzgebieten erfordert relativ hohe zeitliche Auflösungen. Luftbilder und daraus abgeleitete bildbasierte Punktwolken bieten eine Alternative, Oberflächenmodelle zu erstellen. Diese Daten werden in kürzeren Intervallen aufgenommen, wie etwa jährlich in Wien oder flächendeckend für Osterreich alle drei Jahre. Vor allem in Gebieten mit hoher Vegetationsbedeckung wie Wälder führen die beiden Modellansätze zu unterschiedlichen Höhenwerten. Das Ziel dieser Arbeit ist es, diese Unterschiede zu quantifizieren und Möglichkeiten zu eruieren, die Image Matching (IM) Modelle an die ALS Modelle anzunähern.

Zur Entwicklung und Evaluierung eines solchen Prozesses zur Minimierung der Höhenunterschiede wurde ein Gebiet innerhalb des Wienerwaldes im Bereich des Lainzer Tiergartens ausgewählt. Zunächst wurden aus den gegebenen Punktwolken der beiden unterschiedlichen Verfahren topographische Modelle, wie das normalisierte digitale Oberflächenmodell (nDSM), abgeleitet und innerhalb einer eigens definierten Kronendach-Maske statistische Parameter für verschiedene Kernelgrößen des IM nDSM berechnet. Diese Parameter wurden zusammen mit der bekannten Abweichung zwischen dem ALSund IM-Modell verwendet, um eine Random Forest Regression für die Erstellung eines

Anpassungsmodells der IM an die ALS Daten zu trainieren.

Die Validierung, durchgeführt anhand dreier separat definierter Gebiete, zeigt eine Annäherung der Höhenwerte an das als Referenz verwendete Laserscanning-nDSM innerhalb der mit Baumkronen überschirmten Flächen. Diese Verbesserung zeigt eine Annäherung der beiden Modelle von etwa 77% bezogen auf den Median der Abweichungen zwischen dem angepassten und dem gegebenen Modell gegenüber der Ausgangssituation. In langgezogenen Lücken im Kronendach stößt die in Python implementierte Regressionsfunktion an ihre Grenzen und ist daher nicht in der Lage, die im IM-Modell nicht erkennbaren Lücken in bewaldeten Gebieten adäquat an das Laserscanning-Modell an diesen Stellen anzupassen.

# **Abstract**

Airborne laser scanning (ALS) point clouds are employed throughout the country for the generation of digital surface models and to derive further information about forested areas. This acquisition method is considered state-of-the-art up to now, especially in forested areas. However, as these are regularly but not frequently collected in Austria and Europe, modelling based on ALS data of forest parameters in high temporal resolution is difficult. In particular, the derivation of dynamic information such as biomass or condition of a tree population after environmental events such as storms or forest fires or the monitoring of protected areas requires relatively high temporal resolution. Aerial images, along with image-based point clouds derived from them, provide a further option for the creation of surface models. This data is recorded at shorter intervals, such as annually in Vienna or every three years for the entirety of Austria. Especially in areas with high vegetation cover such as forests, the two modelling approaches yield different elevation values. The aim of this study is to systematically quantify these differences and to investigate strategies to approximate IM models to the ALS models.

For this investigation, a specific area within the Wienerwald, in the area of the Lainzer Tiergarten, was selected for the development and evaluation of such a process to minimise the height differences. Initially, topographic models, such as the normalised digital surface model (nDSM), were derived from the available point clouds. Statistical parameters for different kernel sizes of the image matching nDSM were then calculated within a specially defined canopy mask. These parameters, along with the known deviation between the laser scanning and image matching model, were used to train a random forest regression to create a model to fit the image matching with the airborne laser scanning data.

**TU Sibliothek**, Die approbierte gedruckte Originalversion dieser Diplomarbeit ist an der TU Wien Bibliothek verfügbar wern vour knowledge hub. The approved original version of this thesis is available in print at TU Wien Bibliothek.

The validation, conducted on three distinct areas, showed an approximation of the elevation values to the laser scanning nDSM utilised as a reference within the canopy mask. This improvement demonstrates a remarkable approximation of the two models of about 77% in relation to the median of the deviations between the adjusted and the given model compared to the initial situation. The image matching data shows its limitations in elongated gaps in the canopy, as the closing effects of small canopy gaps in forested areas pose challenges for the matching of the images. In such instances, the regression function cannot make any improvements.

# **Contents**

Lis	st of	Figures		xiii
Lis	st of	Tables		χv
1	Intro	oductio	n	1
	1.1	Object	ive of this study	3
2	Stud	ly area	and data	5
	2.1	Study	area	5
		2.1.1	Area of interest	6
	2.2	Forest	definition	8
	2.3	Data		9
		2.3.1	Airborne laser scanning data	10
		2.3.2	Image matching data	10
		2.3.3	Height correction within the ALS products	11
		2.3.4	Digital Terrain Model	15
3	Met	hods		16
	3.1	Data p	preprocessing	16
		3.1.1	Elimination of outliers within the ALS data set	16
		3.1.2	Elimination of outliers within the IM data set	18
	3.2	Topog	raphic model generation	19
		3.2.1	Digital surface model	20
		3.2.2	Normalised height products	21
	3.3	Compa	arability of ALS and IM Data	21
		3.3.1	Fractional Cover and degree of crown coverage	22



		3.3.2	Delineation of forest area	22
		3.3.3	Crown height / tree height	23
	3.4	Rando	m forest regression	24
	3.5	Rando	m forest regression - Validation	28
4	Resi	ults		29
	4.1	Topog	raphic products	29
	4.2	Rando	m forest regression	33
		4.2.1	Kernel sizes / maximum depth	33
		4.2.2	Testing: Number of Estimators / maximum depth	35
		4.2.3	Minimum median regression	38
		4.2.4	Minimum mean regression	43
		4.2.5	Minimum RMSE regression	46
	4.3	Valida	tion results	50
		4.3.1	Validation: Area 1	50
		4.3.2	Validation: Area 2	55
		4.3.3	Validation: Area 3	58
5	Disc	cussion		65
6	Con	clusion		69
7	Refe	erences		72
8	Арр	endix		84

# List of Figures

1	Overview AOI	7
2	Measured heights and reference points	12
3	Height-transformation parameters Austria	14
4	Flowchart outlier cleaning process ALS	17
5	Visualisation of outliers within the ALS point cloud	18
6	Visualisation of the degree of crown coverage	23
7	Normalised surface models of the training area	30
8	Height differences within the training area	32
9	Heatmap of different kenel sizes and maximum depths	34
10	Heatmap of different numbers of estimators and maximum depths	36
11	Representation of single tree heights within the test area. Minimum median	
	random forest regression	39
12	Canopy height plot of the median minimising random forest regression model.	41
13	Histogram of height deviations within the median minimizing model	42
14	Representation of single tree heights within the test area. Minimum mean	
	random forest regression	44
15	Canopy height plot of the mean minimising random forest regression model.	45
16	Histogram of height deviations within the mean minimising model	46
17	Representation of single tree heights within the test area. Minimum RMSE	
	random forest regression	47
18	Canopy height plot of the RMSE minimising random forest regression model.	48
19	Histogram of height deviations within the RMSE minimising model $\ \ldots \ \ldots$	49
20	Histogram of height differences in validation area 1	50
21	Plot of the adjusted IM nDSM and the difference image in validation area 1.	53

22	Canopy height plot: Validation area 1	54
23	Histogram of the height differences in validation area 2	56
24	Plot of the adjusted IM nDSM and the difference image in validation area 2.	56
25	Canopy height plot: Validation area 2	58
26	Histogram of the height differences in validation area 3	59
27	Plot of the adjusted IM nDSM and the difference image in validation area 3.	60
28	Canopy height plot: Validation area 3	62
29	Mean deviation and frequency before and after the random forest adjustment	64

# List of Tables

1	Metadata for defined areas within the AOI	8
2	Measured height reference points	12
3	Summary of the three best models in the training process	37
4	Statistical parameters of the first validation area	51
5	Statistical parameters of the second validation area	57
6	Statistical parameters of the third validation area	61

# 1 Introduction

Forests have a central function in society and play an important role not only for the global climate, but they also serve as a habitat for countless animals and plants. They also contribute to the regulation of water cycles and carbon storage. Above all, the forest is a place of recreation for humans (Ranacher et al., 2023).

For this reason, the protection and conservation of biodiversity of forests play a central role not only regionally, but also Europe-wide (please refer to Umweltbundesamt (n.d.)). The success of the protection of these areas can be proven by active monitoring as described by Ceccherini et al. (2023). Monitoring has a major importance not only in a global perspective, but also for forestry applications across national territories (Goodbody et al., 2021) as well as at smaller regional scales (Puliti et al., 2020).

To obtain information on resources and on the condition of, as well as changes in, the forest ecosystem, so-called forest inventories are carried out (BFW, 2022). These inventories are not only performed manually by experts on site (BML, n.d.) which can only be conducted for a couple of chosen areas. To overcome such spatial limitations data is increasingly generated by using remote sensing technologies (further information e.g. White et al., 2016). For example, airborne laser scanning (ALS) data is often used for the purpose of monitoring forest growth heights (Yu et al., 2004; Næsset & Gobakken, 2005). In Austria, the Austrian Federal Forestry Office (OBf) is also testing the use of drones, laser scanning and artificial intelligence for digital forest inventories (OBf, 2023).

ALS, often also referred to as LiDAR (Light Detecting And Ranging), is an active remote sensing method, where laser scanners are mounted on a helicopter or aircraft as described by Pfeifer et al. (2007). In more recent applications, scanners are also mounted on socalled UAVs, unmanned aerial vehicles (Puliti et al., 2019). In ALS, intense, focused

beams of light are emitted from a scanner (transmitter). A sensor (receiver) records the reflections of the beam from the surface. The collected information, in this case, the travel time, is used to calculate ranges. In the case of ALS, the distance from the sensor to the object on Earth is derived. With this information, coordinates can then be calculated when the position of the laser scanner is known. (NOAA, 2012)

The advantage of using full waveform (FWF) ALS, as described by Hollaus et al. (2014), is that the number of detected reflections (echoes) is not limited to the first and last echo. The entire waveform is recorded and allows the description of the entire canopy profile within one acquisition. However, not only changes in the forest area can be detected using ALS, but also changes in the urban area (Murakami et al., 1999; Tran et al., 2018). This approach can also be used to detect damage on buildings (see Rastiveis et al., 2018).

As forests are a dynamic and not rigid system, numerous recordings are necessary for monitoring the actual situation without temporal gaps. In the past, the ALS acquisitions in Austria were not organised nationwide, but were carried out by the individual federal states themselves. The frequency of collecting and providing nationwide DSMs is six to ten years. Now, they are organised nationally by the Federal Office of Metrology and Surveying (BEV). BEV specifies an update interval of 3 years for the digital surface model (DSM) created from IM data (BEV, 2019). In Vienna, aerial photographs are taken annually over the entire city (Stadt Wien - Stadtvermessung, n.d.) and thus, these images have a high potential to fill temporal gaps between ALS data acquisitions.

As an alternative to ALS data, 3D information can also be derived from aerial images using photogrammetric reconstruction methods. Since the inner orientation (IOR), principal distance, principal point and lens distortion as well as the exterior orientation (EOR) with spatial location and rotation of the image are known, a point cloud can be generated by spatial intersection of viewing rays between pixels within the aerial images (Ressl et

al., 2016). These IM point clouds can be utilised for various monitoring tasks. Similar to ALS, forest parameters and changes can be derived from these point clouds (see Navarro et al., 2018; Ali-Sisto & Packalén, 2017).

Temporal augmentation of data from aerial photography and its derived point clouds can be used to gather information after forest fires. Since this process is predominantly carried out using ALS data (Casas et al., 2016; Viana-Soto et al., 2022), it is presumed that an ALS dataset is available precisely at or subsequent to this point in time.

## 1.1 Objective of this study

Particularly in areas where aerial imagery is acquired on a regular basis and ALS acquisitions are made only at longer intervals, IM may offer a way to provide additional and comparable data. There are differences regarding the height values between the two acquisition methods, IM and ALS, in their point clouds and the derived parameters (Ullah et al., 2017). This leads to the research question of whether it is possible to minimise differences in the derived normalised surface models.

Especially in regions where aerial images are regularly taken and ALS surveys are carried out at longer intervals, IM can offer a cost-efficient and flexible way (Honkavaara et al., 2013) to obtain comparable data. Given the observed differences in elevation values between the two acquisition methods IM and ALS in their resulting point clouds and derived parameters, the question arises if these differences can be minimised in the resulting normalised surface models.

This thesis addresses the main objective of minimising height differences resulting from different acquisition methods such as IM and ALS. The main focus lies on investigating whether and how these differences are influenced by different forest structures, including

both unmanaged and actively afforested areas. The aim of the study is to analyse these differences using only IM data.

The methodology outlined in this thesis not only provides the potential for improved temporal resolution but could also provide the basis for standardised comparability of terrain models, regardless of the different technological approaches to data acquisition.

By analysing these objectives, this thesis not only aims at overcoming existing challenges related to elevation differences, but also at developing innovative solutions that contribute to improved temporal resolution and consistency of terrain models within forest areas obtained using different imaging techniques.

# 2 Study area and data

For carrying out various calculations and producing different results, an area of interest (AOI) had to be defined. The area of interest used in this study is highly diverse in terms of forest management aspects. There are actively managed forestry areas as well as unmanaged, protected areas with no active human intervention.

## 2.1 Study area

Since the Wienerwald is located in and around Vienna, and as it has a coverage of both data (ALS and IM) at close temporal recording dates, an area of the Biosphere Park Wienerwald was selected as the area of interest for this thesis.

### Biosphärenpark Wienerwald

In 2005, Wienerwald was designated a UNESCO biosphere park as one of around 700 regions in 134 countries around the world (UNESCO, 2021) due to its unique diversity of natural and cultural landscapes and making it one of four such biosphere parks in Austria. In its full size, the biosphere park has an area of 1056.45 km<sup>2</sup> (which corresponds to 5.4% of the total area of Vienna and Lower Austria) and encompasses 51 Lower Austrian municipalities and seven Viennese districts and plays an important role not only for the people who live there, but also for society, landscape and life in eastern Austria. Biosphere reserves are areas which are founded for reasons of a special protection or development concepts to guarantee an optimal balance between the protection of biodiversity and economic as well as social development while upholding important cultural values and traditions (Biosphärenpark Wienerwald Management GmbH, 2020).

### 2.1.1 Area of interest

Within this region of Wienerwald, an area located in the  $13^{th}$  Viennese district (Hietzing) in the northern part of Lainzer Tiergarten, including the area of Johanneser Kogel (the outline is shown black in Figure 1) located next Auhof was defined. This area was used to implement a machine learning algorithm to align IM height values to ALS heights for increasing temporal resolution of forest parameters.

In the designated region, one of 37 so-called "Kernzonen" (core zones) of the Wienerwald Biosphere Reserve is located. This core zone, Johannser Kogel, is part of these areas which are particularly protected. Within these sub-areas, the primary purpose is to preserve the original habitats extensively as possible and thus to protect the unique symbiosis between rare plants and animals from human intervention. The Johannser Kogel benefitted from this protection since 1972 and has not been used for forestry purposes since then. Since there is no human intervention, a natural cycle is created which is not (actively) influenced by humans and which makes it possible for the "primeval forest of tomorrow" to grow up (Biosphärenpark Wienerwald Management GmbH, n.d.).

The area used for training the random forest algorithm inside the AOI is delineated by a red rectangle in Figure 1. In this area, both uncovered and canopy covered areas which show different characteristics related to the height when looking at the aerial images, can be found. As stated by Brugisser et al. (2021), who also used some parts of the Wienerwald for his research, the dominating species in this region are beeches, oaks and hornbeams. In the south-eastern area of the main AOI used for training the random forest regression, an area with visible human influences, straight forest aisles can be found. These characteristics indicate active management of the forest.

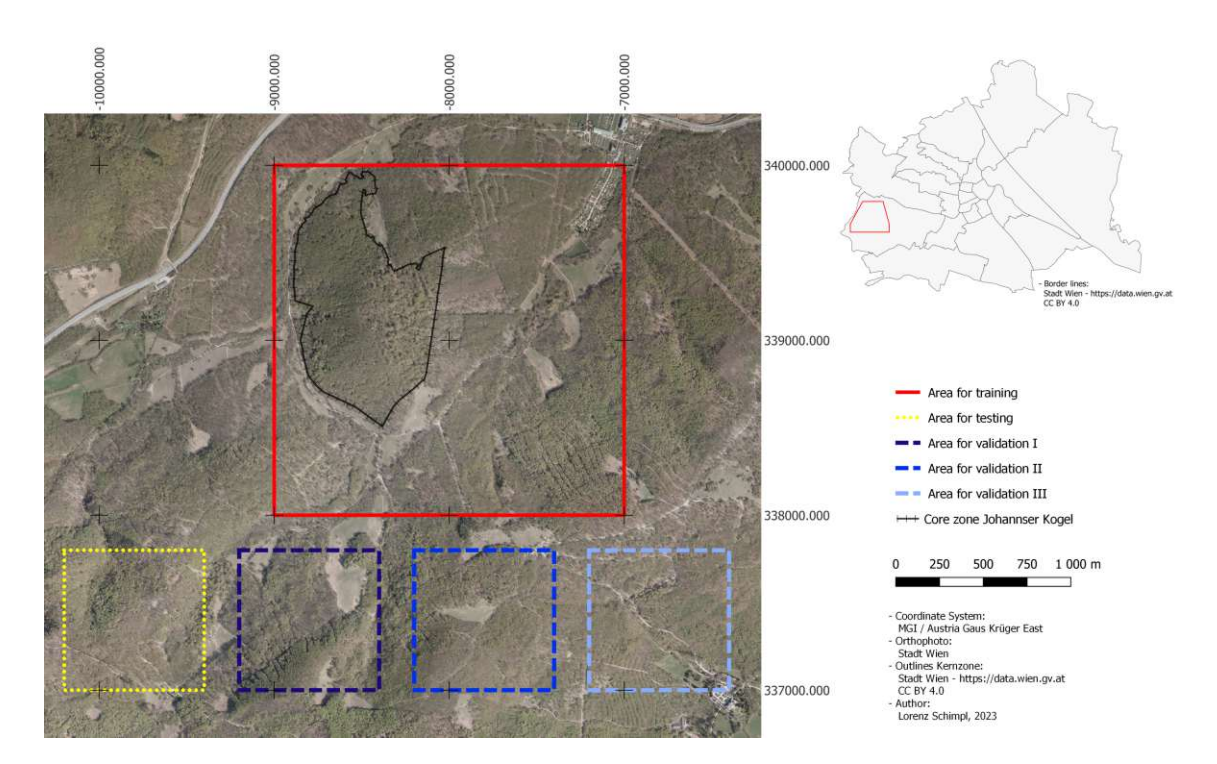


Figure 1: Overview of the AOI, including the core zone Johannser Kogel (black). Differentiation between training area (red), test area (yellow dotted) and the three validation areas (blue) in the area of Lainzer Tiergarten in the  $13^{th}$  Viennese district. Austria GK East. EPSG: 31256

For the later performed random forest regression a test area (yellow rectangle) as well as three validation areas (blue rectangles) located in the south of the AOI, were defined. Table 1 provides details on the geographical location and extent of the area. Those testand validation subsets, each cover an area of 0.64 km<sup>2</sup>, share similar characteristics with the originally defined training area. Within these designated test and validation subareas, the vegetation is similar to the one in the training area. In addition to a densely filled canopy, elongated gaps in the canopy can also be recognised. The type of vegetation (deciduous forest) is the same as in the training process. Within these four sub-areas there is no explicitly defined core zone as in the training area.

Tab. 1: Defined areas with their upper left coordinates, extent in East and South direction CRS: MGI / Austria GK East. EPSG: 31256 as well as their surface area.

Name	X [m]	Y [m]	Extent East [m]	Extent South [m]	Area [km <sup>2</sup> ]
Training	-9000	340000	2000	2000	4
Testing	-10200	337800	800	800	0.64
Valid I	-9200	337800	800	800	0.64
Valid II	-8200	337800	800	800	0.64
Valid III	-7200	337800	800	800	0.64

### 2.2 Forest definition

The definition of forest is very variable and varies between countries (Venkateswarlu, 2013) but also within countries for different applications. As a result, there are around 1000 different definitions worldwide for such a common-day topic, as described by Lund (2016). (Note: There are 193 member states of the United Nations worldwide (UNRIC, 2019))

The European definition, established by the Food and Agriculture Organisation of the United Nations, defines forest for its Sustainable Development Goals (SDG) (for more information see: United Nations, 2023; BMEIA, n.d.) as:

"Land spanning more than 0.5 hectares with trees higher than 5 meters and a canopy cover of more than 10 percent, or trees able to reach these thresholds in situ. It does not include land that is predominantly under agricultural or urban land use"

(United Nations, 2023)

In Austria, the definition of forest differs from the European Union concept. For instance, in Austria, the term forest (Wald) is described in the Forest Act (Forstgesetz) of 1975 as followed:

"Forest within the meaning of this Federal Act consists of basal areas stocked with woody plants [...], where the growing stock reaches an area of at least 1000 m<sup>2</sup> and an average width of 10 m."

(§ 1a Abs. 1 Forest Act 1975)

The Austrian National Forest Inventory (Österreichische Waldinventur - ÖWI) has its own definition for the survey of forests in Austria. Here it is specified that a forest is to be recorded as such if it consists of an area of woody plants with a minimum area of 500 square metres and a minimum width of 10 m. The minimum canopy cover, in other words how much surface is shaded by the crowns, must be at least 3/10, or 30\%, as stated by OWI. (Hauk et al., 2020)

### 2.3 Data

For the later performed calculations, ALS data as well as IM point clouds from aerial photographs were used. In order to ensure adequate comparability of the two point clouds, it was necessary to find a data pair acquired in the same year with a comparable phenological status. This condition was taken into consideration to enable precise analysis and evaluation within the scope of this thesis.



### 2.3.1 Airborne laser scanning data

The dataset used for this thesis, also used by Mandlburger et al. (2019) and Bruggisser et al. (2021), captures an area of 53 by 8 km, generated by 18 strips with an overlap perpendicular to the flight direction of 50%. Within this flight campaign, great parts of the City of Vienna, were measured by a Riegl VQ-1560i (RIEGL Laser Measurement Systems, Horn, Austria) full waveform LiDAR (Light Detecting And Ranging) scanner on September  $20^{th}$  in 2018 under leaf-on conditions.

The average flight altitude was 750 m above ground at a flight speed of 216 kilometres per hour and a pulse repetition rate of 1.33 MHz. For capturing the area, two independent laser channels with a wavelength of 1064 nm within the scanner where used (Bruggisser et al., 2021). In the area for testing and validating the random forest regression, the average point density refers to 81 echoes per square meter.

### 2.3.2 Image matching data

The IM point cloud including metadata and processing information was provided by the Federal Research and Training Centre for Forests, Natural Hazards and Landscape (BFW) for further processing within the SeMoNa Project (Iglseder et al. 2023). This dataset was also used for creating and working on the algorithm in this thesis.

As stated by Iglseder et al. (2023), aerial photographs acquired with a ground sampling distance (pixel size on the ground) of at least 0.2 m was acquired with an Ultracam Eagle Mark 2 from Vexcel on August the  $8^{th}$  in 2018. The point density refers to 25 points per square meter. To produce the images an overlap of 80% in the direction of flight and a minimum overlap of 30% perpendicular to the direction of flight was used.

The point cloud was created using Trimble's MatchT software. For each pixel within the



image, from the best image pair, a point was created with x, y, z coordinates and RGBI values. All available images are used as long as there is at least 80% overlap in flight direction.

### 2.3.3 Height correction within the ALS products

ALS and IM data are both presented in different elevation systems: the ellipsoidal heights (ALS) and the Gebrauchshöhe (IM). To enable a comparison between the two data sets, the ellipsoidal heights of the ALS data are converted to the Austrian Gebrauchshöhe, which is the common elevation system used in Austria. The Austrian Gebrauchshöhe is referred to the average Adriatic sea level in Trieste from 1875 (for more information see BEV (n.d.-a). This height system was directly used in the IM data set. To assess the initial height differences and the accuracy of the following conversion, five different height control points (see Figure 2) were selected within the training area at locations not covered by high vegetation. These surface control points were assumed to be equal to the terrain height.

The calculated difference at the selected points showed an average difference of approximately +44 m in height in the ALS model compared to the IM. In order to verify the heights, the non-normalised surface heights (altitudes given as metres above Adriatic sea level) were requested from the geodata viewer (Geodatenviewer, available at: https://www.wien.gv.at/ma41datenviewer/public/) of the City of Vienna at the previously selected reference positions without high vegetation.

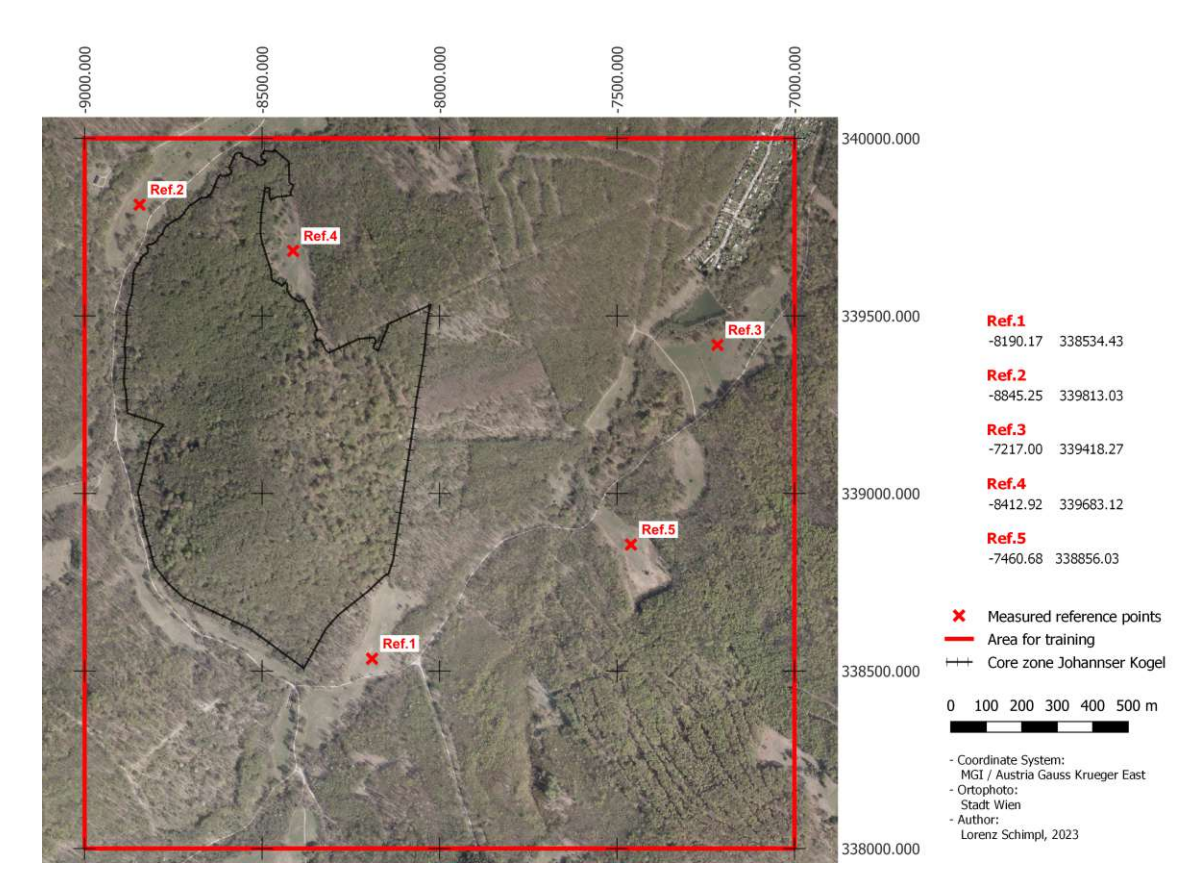


Figure 2: Representation of the reference points measured from the digital surface model (DSM) of the ALS campaign, the IM data and the reference value from the Geodatenviewer of the City of Vienna within the area used for training the random forest regression.

Tab. 2: Comparison of heights in metres above Adriatic sea level at different reference points in relation to image matching (IM), airborne laser scanning (ALS), reference heights of the City of Vienna (REFERENCE) and the height values after adjustment with the height grid (ALS BEV).

Reference point	Ref. 1	Ref. 2	Ref. 3	Ref. 4	Ref. 5
IM height [m] ALS height [m]	301.9 346.3	245.0 291.7	251.5 296.1	275.1 319.5	280.2 324.8
Height difference [m]	44.4	46.7	44.6	44.4	44.6
ALS BEV height [m] REFERENCE height [m]	301.5 301.7	247.0 247.0	251.4 251.6	274.8 274.9	280.0 280.2
Height difference [m]	0.2	0.0	0.2	0.1	0.2

As illustrated in Table 2, the height shift of around 44.9 m in the ALS compared to the



reference values of the points in the Geodatenviewer can be confirmed. After applying the height transformation from ellipsoidal heights to Gebrauchshöhe, the average deviation to the reference values could be reduced to a mean value of under 0.1 m.

The height differences between the ellipsoidal heights within the ETRS89/GRS80 system and those used in Austria, referencing the mean sea level of the Adriatic Sea in 1875 in Trieste according to the Military Geographic Institute (MGI), are described by the "Höhen-Grid plus Geoid" (BEV, n.d.-b). With the height differences provided the ellipsoidal heights can be adjusted as described by BEV (n.d.-b) in Equation 1.

$$H_{gebr(niv)} = H_{ell} - \Delta H_{HGridplus} \tag{1}$$

with:

 $H_{ell}$  [m] ellipsoidal height related to the GRS80 ellipsoid

 $H_{qebr(niv)}$  [m] "Gebrauchshöhen" adapted to levelling

 $\Delta H_{HGridplus}$  [m] interpolated height difference calculated from height grid

plus Geoid

As described by BEV (n.d.-b), height differences have a resolution of 15 by 22.5 arc seconds. As can be seen in Figure 3, the required correction values increase in mountainous areas compared to flat areas. The accuracy of the correction values for height also decreases in the mountains, resulting in an accuracy of the correction parameters of approximately  $\pm$  0.035 m in flat areas and around  $\pm$  0.06 m in mountainous regions which need to be considered when working with re-projected datasets.



Applying the transformation to the ALS data in this thesis, Equation 1 can be described as follows. The height correction grid of BEV is subtracted from the DSM generated from the ALS point cloud in the ellipsoidal height system GRS80, and the systematic error can effectively be removed.

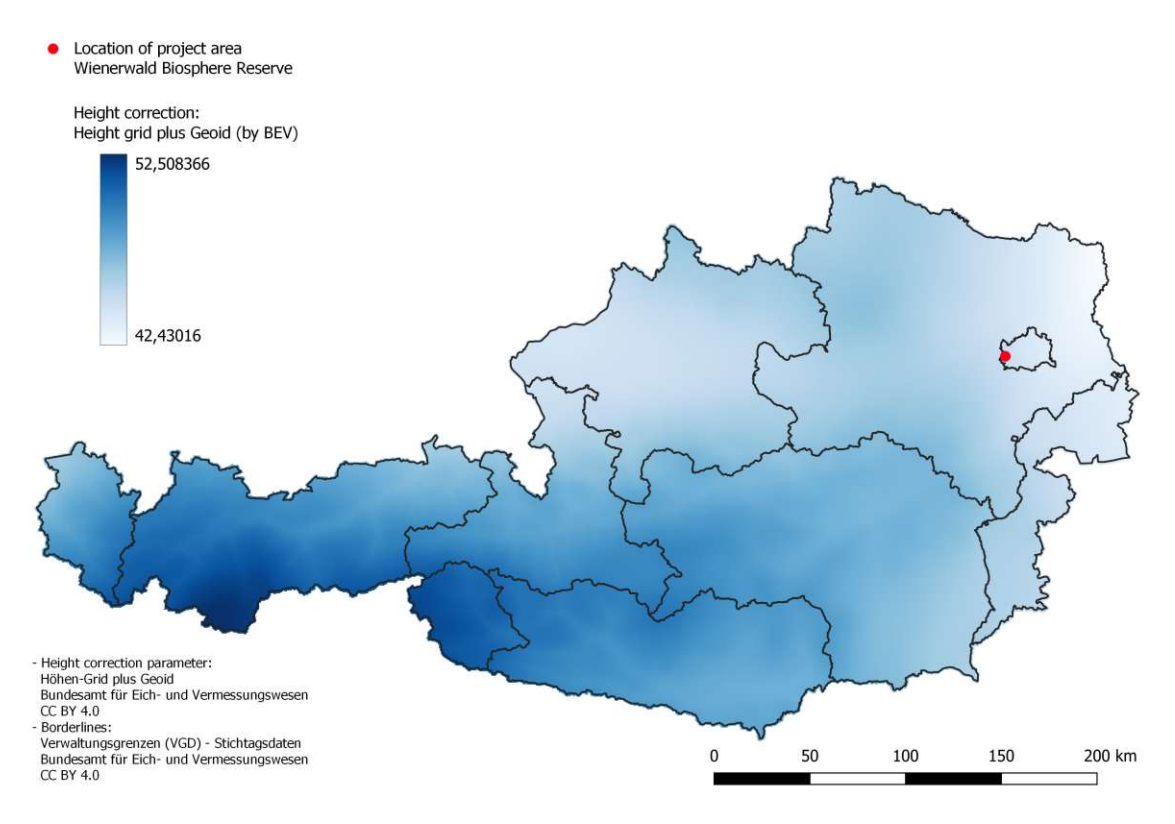


Figure 3: Visualisation of the height correction for transformation of ellipsoidal heights into the heights above the Adriatic sea used in Austria (MGI). The red dot indicates the location of the project area in Vienna.

### 2.3.4 Digital Terrain Model

The digital terrain model (DTM) used in this study was created by the City of Vienna. This model has been updated on a quarterly basis since 2015 with an original spatial resolution of 0.25 by 0.25 m, generated using airborne laser scanning. For further processing within the SeMoNa project, the raster size was resampled to a cell size of 0.5 m and was also used for the calculations performed later in this thesis. The original raster data for the terrain of the City of Vienna is available via the Kund\*innen-Servicestelle -Stadtvermessung (https://www.wien.gv.at/stadtentwicklung/stadtvermessung/ geodaten/produktvertrieb.html)

# 3 Methods

## 3.1 Data preprocessing

### 3.1.1 Elimination of outliers within the ALS data set

The ALS point cloud used in this study was not yet cleaned from outliers. Therefore, a consistent algorithm was developed that could be applied to different types of point clouds. For the following calculations, the point cloud processing software package OPALS (Pfeifer et al., 2014) developed by the Department of Geodesy and Geoinformation - Research Groups Photogrammetry and Remote Sensing at TU Wien was used.

As the calculation of the (normalised) surface models within the ALS data revealed implausible values, a way of removing such elements from the point cloud had to be implemented. As visualised in Figure 4, all points classified as outliers before the data was provided by RIEGL (see red dots in *Figure 5*) were previously excluded by a filter. Points which had a classification other than 64 (outlier) were taken directly to the next adjustment phase.

Afterwards, a 1 by 1 m grid was calculated from the previously cleaned point cloud. As feature for generating this grid, the value of the 98<sup>th</sup> quantile of the Z-values for the point cloud was calculated in each such 1 m cell. The resulting simplified surface model of the  $98^{th}$  quantile was used in the following step as a grid file to determine the distances between the  $98^{th}$  quantile surface model and the points in the point cloud.

The new attribute (DSM) added to the point cloud could then be filtered again. Any point with a distance of more than 2 metres between the grid file and the corresponding point (blue points in *Figure 5*) in the following filtering process was again excluded from the point cloud.

The remaining elements (grey points in Figure 5) of the ALS point cloud could then be used for further processing steps and the derivation of topographic elements.

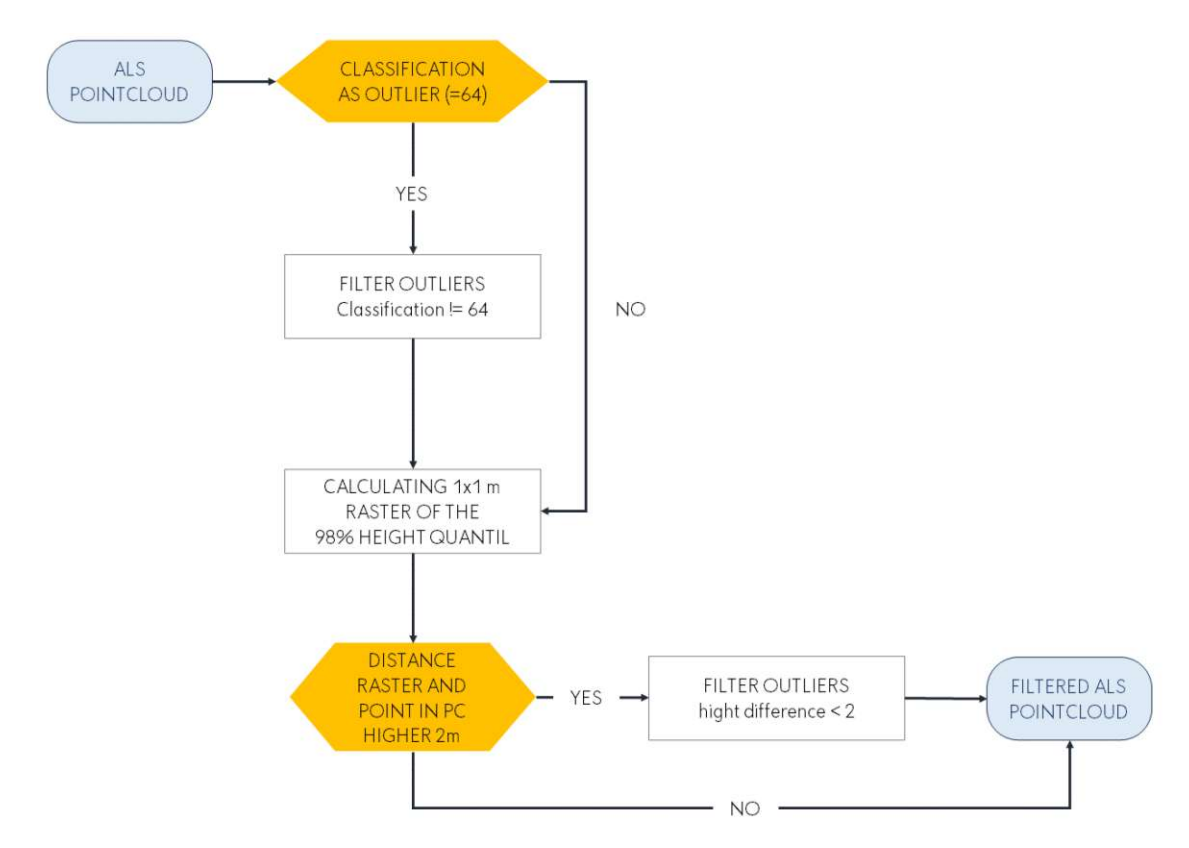


Figure 4: Workflow of the filtering process within the ALS data. The yellow boxes represent decision points in the flowchart, while the rectangular boxes represent the execution of specific steps.

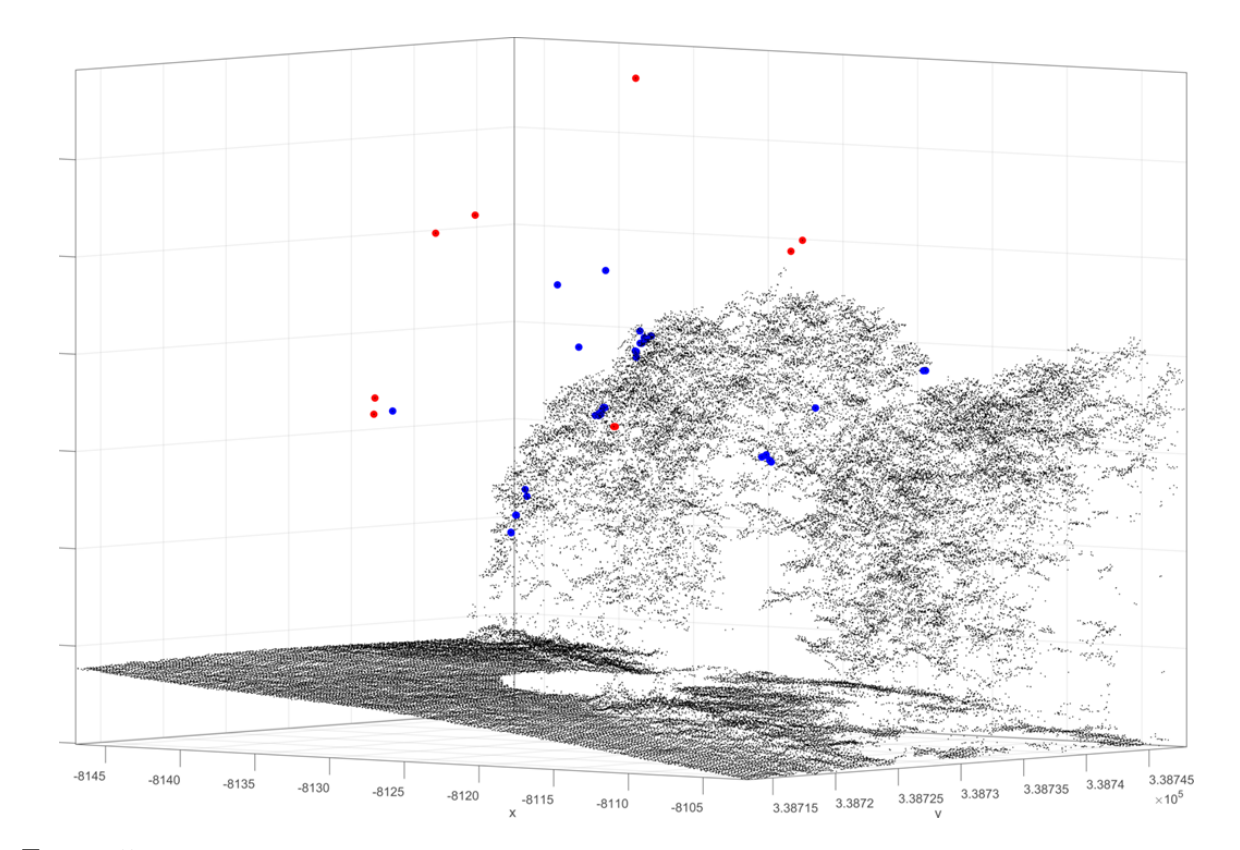


Figure 5: Representation of the ALS point cloud in a 45 m by 35 m large field around the center coordinates: -8124.42 m / 338730.52 m (CRS: MGI / Austria GK East; EPSG: 31256). The red points are those which have previously been classified as outliers, with a classification of 64. Points in blue are points that have the threshold value higher than 2 m in the newly created attribute (\_DSM) and are therefore also treated as outliers.

### 3.1.2 Elimination of outliers within the IM data set

As stated in (Chapter 2.3.2), no further outlier elimination was applied due to the BFW in-house developed Python code by Aufreiter & Schöttl for this purpose:

- Dividing the point cloud into 5 height levels. Heights above 60 m are treated as outliers.
- Clustering points in levels 2, 3 and 4 using Density-Based Spatial Clustering of Applications with Noise (DBSCAN)

- Small clusters detected by DBSCAN with less than 5 points are flagged as outliers.
- Calculation of the distance from the cluster to the nearest 25 neighbours is performed twice.
- Outliers from level 3 and 4 detected by DBSCAN are checked whether their distance to the nearest 20 neighbours is lower then 2 m.

In this algorithm, the point cloud was first divided into height layers. Points with a height of more than 60 m in the canopy height model (CHM) were classified as errors and removed without further consideration. The other 4 layers are defined by the  $99^{th}$ percentile of the CHM height (layer 4) and a 1 m buffer below this layer (layer 3). Below layer 3 there is another buffer zone, layer 2. No processing is performed for points in the lowest layer, so possible outliers in this area are not treated.

Points in the individual layers are clustered and classified as clusters or outliers. Smaller clusters, from layers 3 and 4, with a number of points below 5 are classified as outliers. For the remaining ones, the median of the coordinates is calculated. Afterwards, the remaining clusters are checked based on a distance and spectral criterion to see whether they are outliers or remain within the point cloud. (Aufreiter & Schöttl, 2019)

# 3.2 Topographic model generation

To visualise the point clouds and generate data for the random forest regression in an improved way, digital surface models were calculated to switch from a point-based to a pixel-based approach.

## 3.2.1 Digital surface model

The processing steps described in this and the following chapters were applied to both, the ALS- and the IM generated point clouds in the same way.

For the calculation of the DSM again OPALS was used. The DSM, according to Hollaus et al. (2010) represents the topmost surface which can be seen from the acquisition platform. The algorithm implemented in this software is a combination of two different DSM generation methods. This method was invented and described by Hollaus et al. (2010) and combines the DSM<sub>max</sub> which uses the highest value within a defined cell and the  $DSM_{mls}$  which is based on a moving planes interpolation.

The same input parameters were chosen for both point clouds to achieve comparable results. The grid size, the size of the square grid pixels of the resulting DSM, was set to 1 m. The maximum search radius for the point selection for the DSM calculation, the radius which specifies the range in which points are used for the interpolation of the  $DSM_{msl}$  (OPALS, 2016-a), was set to 5 times the cell size.

The search for neighbours within the DSM calculation with OPALS is a raster-based process. First, a regular grid is created that has half the targeted grid (cell) size (in this case 0.5 m) and the maximum height is stored in each cell. Valid cells (it contains at least one point) are searched for within a defined search radius. To calculate the moving planes approach for rough areas of the point cloud, the previously defined number of neighbours for the interpolation is searched for each grid point. If the number of valid neighbours is not reached, the search radius (by default 3 times the cell size) is extended step by step until either the required number of neighbours or the maximum search radius is reached. For the interpolative approach, the DSM height is calculated using moving least squares interpolation (OPALS, 2016-a; Hollaus et al., 2010).

# TU **Bibliothek**, Die approbierte gedruckte Originalversion dieser Diplomarbeit ist an der TU Wien Bibliothek verfügbar wien knowledge hub. The approved original version of this thesis is available in print at TU Wien Bibliothek.

### 3.2.2 Normalised height products

Another product calculated from the previously created DSMs relates to the normalised heights in the area of interest. The normalised DSM (nDSM) provides terrain feature heights with respect to ground (Rao et al., 2022). In open areas, without vegetation and buildings such as grassland or streets, the DSM and DTM are equal and thus the normalised surface model is zero (Hollaus et al., 2010).

In forestry terminology, this product is also referred to as the canopy height model (CHM) (Liu & Dong, 2014) and describes the height of the tree crowns in relation to the underlying DTM (Hollaus et al., 2010).

The DTM described before in *Chapter 2.3.4*, is used for both acquisition methods when calculating derived parameters such as the nDSM or CHM. This ensures comparability between the absolute heights obtained within this analysis.

$$nDSM = DSM - DTM \tag{2}$$

The normalised DSM can be calculated as shown in Equation 2, by just subtracting the DTM from the DSM.

# 3.3 Comparability of ALS and IM Data

The objective of this research is to develop an area-based approach for enhancing the comparability of canopy heights. Thereby, a higher temporal resolution of forest structure parameters should be achieved. For this purpose, a mask of the canopy is created from the previously calculated nDSM, which is then used to calculate statistical characteristic canopy properties based on the height values of each pixel regarding its local

neighbourhood. This information serves as the basis for training of the random forest regression which was implemented and trained in a python program developed within this research.

## 3.3.1 Fractional Cover and degree of crown coverage

To describe the fraction of ground covered by forest canopy within a defined area (Bruggisser et al., 2021), an approach based on Morsdorf et al. (2006) using the canopied area and the total area under investigation was implemented. For the calculation of the fractional coverage, *Equation 3* has been applied.

fractional cover 
$$[\%] = (\frac{canopy\ area\ [m^2]}{total\ area\ [m^2]}) \cdot 100$$
 (3)

For the fractional cover index described in Equation 3, it was necessary to define what is considered as forested area. As described in *Chapter 2.2*, there are many definitions for the term forest. For the calculation of this index within this work, the following procedure was therefore applied to define the canopy area.

### 3.3.2 Delineation of forest area

The determination of the canopy area is run pixel wise. For this purpose, a binarisation of the nDSM was previously performed. Those pixels with a nDSM value higher than 2 m were set to one and the remaining ones, below this threshold were set to zero. From this binary map, the degree of crown coverage was calculated using a pixel-wise moving window algorithm with a 3 by 3 cells neighbourhood.

The result of the calculated canopy cover is visualised as a map in Figure 6 with values between 0\%, for open areas such as meadows or fields, and 100\% for areas fully covered by canopy. All pixels that exceed a threshold of 50% are then binarised again - this threshold was later raised to 90% as described in *Chapter 3.4*. After the binarisation, pixels that count as canopy are assigned to a value of one, while those areas that do not fall within the definition of "covered with canopy" are stored as not a number (NaN).

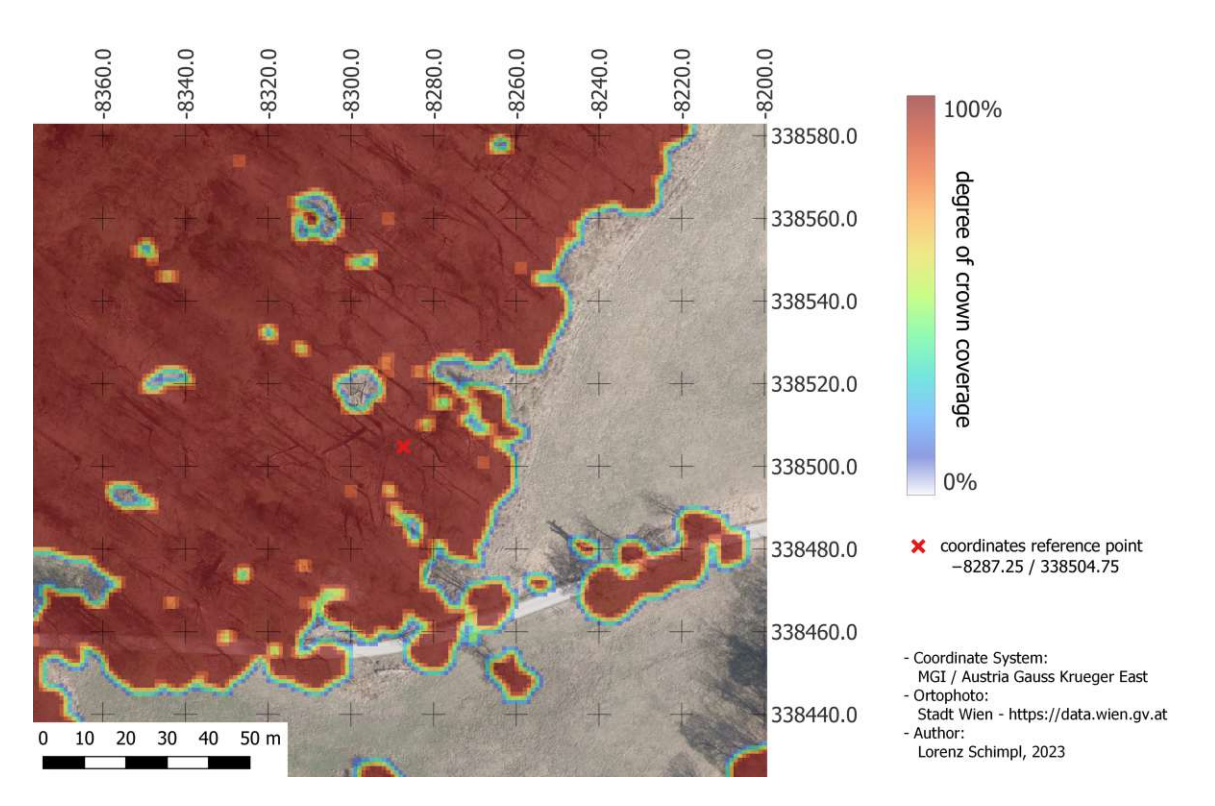


Figure 6: Visualisation of the degree of canopy cover calculated from the IM data set in a subsection of the area for training. Areas without canopy cover are shown transparently as orthophotos.

# 3.3.3 Crown height / tree height

To facilitate a comparison of canopy height distributions and the previously calculated area of canopy-covered pixels, boxplots for different height values both before and after implementing the random forest regression were created. Only the heights of those pixels of the raster image were included in the calculation which fell within the previously created canopy mask with a canopy coverage above 50%.

# 3.4 Random forest regression

The random forest regression model is a supervised machine learning algorithm combining the predictions of multiple decision tree regressors to improve accuracy and robustness. It is based on several input features. After training, tuning and testing a model, independent data was used to validate the performance.

### Feature extraction

The StatFilter module (moving window algorithm) in OPALS employs with raster files such as the previously generated nDSM and calculates statistical features for each pixel by considering the neighbouring pixels in a pre-defined radius / kernel size. (OPALS, 2016-b)

The extracted statistical parameters of the random forest regression are listed below.

 $\rightarrow$  median  $\rightarrow$  mean

 $\rightarrow$  95th quantile  $\rightarrow$  98th quantile

 $\rightarrow$  99th quantile  $\rightarrow$  range

 $\rightarrow$  root mean square error (RMSE)  $\rightarrow$  standard deviation

 $\rightarrow$  median absolute deviation

These statistical parameters were calculated using a moving window and varying kernel sizes in relation to the values of the nDSM over the entire area. The applied kernel sizes in this study were 3x3, 5x5, 7x7, 9x9 and 15x15 pixels.

### **Training process**

The "RandomForestRegression" module developed by sk.learn (sk-learn, n.d.) and implemented in Python was used to perform the random forest regression in this study. Values for adjusting the IM data could be produced using the derived calculated statistical parameters from the nDSM as features and the calculated height difference as the target value.

As described by Beheshti (2022), a random forest regression works with different individual calculated decision trees. These originate from a root and subsequently bifurcate into two new paths at each node, based on the results of variables, until reaching the socalled leaf node - the end of such a tree. As mentioned in this article, there are different parameters which can be set. In the Python implemented sk.learn Module "RandomForestRegression", the number of individual trees, the number of used estimators per node and the maximum depth can be set. An important parameter which needs adjustment mentioned by Beheshti (2022) is the maximum depth. By varying this value, the deepness of such a tree is modified. An important factor to consider when applying random forest models to large datasets is the potentially long training time.

Considering the runtime optimisation, the input data needed to be thinned out due to their size of 2001 by 2001 within the raster image matrix. Only every  $10^{th}$  value of the 4004001 entries was used for the performed random forest regression training. Due to this limitation, the maximum number of features was indirectly set. This is also a possible aspect of the random forest regression hyper parameter tuning.

When conducting the experiment, different settings were used for the following parameters:

 $\rightarrow$  maximum number of estimators

 $\rightarrow$  maximum depth

 $\rightarrow$  kernel size of the input data

To improve the results in the canopy area and due to the fact that the IM-nDSM and the ALS-nDSM are very similar in the open non-vegetated area, the mask previously calculated in *Chapter 3.3.1* was extended and increased to at least 90% canopy cover. This measure was taken to avoid including the edges of the forest in the training of the random forest regression, as significant variations can be observed between the two recording methods. This is because of the large differences between the ALS and the IM model in the edges, which would have a negative influence on the training of the regression function.

At the beginning, the calculations were performed with a kernel size of one, meaning a calculation of the statistical parameters in relation to a neighbourhood of 3 by 3 pixels around every pixel for the input. The kernel sizes used were also expanded to sizes two, three and seven for the later executed testing.

### Hyperparameter tuning

Since the result from a single run does not contain the optimal result, a so-called hyperparameter tuning was implemented. As described by Koehrsen (2019), hyperparameter tuning is based on an experimental basis rather than a reproducible theory.

Within this thesis, the tuning parameters which were varied, were the maximum number of estimators and the maximum depth of the decision trees. The initial training which was carried out, was the variation of the input data, the maximum depth of 5, 10, 20, 30, 40, 50 and unlimited while using 10 estimators.



### Random forest regression - Testing

The testing of the previously trained and tuned regression function was performed using a second developed script on a different data set to avoid overfitting by training and testing on the same data set described by Koehrsen (2018).

To be able to assess the training and its results without getting a problem regarding overfitting, various statistical parameter were calculated in each case for the defined test area outside the training area. The difference between the adjusted IM nDSM ( $IM_{ADJ}$ ) and the actual ALS nDSM (ALS<sub>REF</sub>) within the area was calculated. Based on this difference vectors, again statistics have been computed. One of these parameters evaluated was the Root Mean Square Error (RMSE), also used for assessing random forest regressions by Liu et al. (2020), which is calculated as stated in Formula 4.

$$RMSE = \sqrt{\frac{1}{n} \sum_{i=1}^{n} (y_i - \hat{y}_i)^2}$$
 (4)

Where y stands for the adjusted value and  $\hat{y}$  for the true value. For n, the number of values within the test set is used. Further testing was performed using classic statistical parameters as the mean, median and as well the Pearson Correlation Coefficient (R). As already described and also applied by Balogun & Tella (2022), the Pearson's R value in this thesis was used for evaluating the relationship between the given and the adjusted nDSM model. A combination of all these parameters was used to evaluate the most suitable random forest regression model.

After a kernel size has been identified as the most efficient one in its particular test, further hyperparameter tunings were performed on it. The number of estimators was changed to 10, 30, 50 and 100. The results again were compared by evaluating its individual statistics.



# 3.5 Random forest regression - Validation

To finally validate the previously trained and tested model, three validation areas were defined (see Figure 1). In these areas, the tuned model from the previous test was applied again individually and assessed on the basis of their statistical parameters of the difference between  $(IM_{ADJ})$  and  $(ALS_{REF})$ . Validation in external additional areas offers the possibility of assessing the accuracy of the model in an independent area without reference data.

# 4 Results

In Chapter 4.1 the topographical products and the models derived from them will be presented. In the second part of *Chapter 4.1* the differences concerning the fractional cover of the training area are described. In Chapter 4.2 the outcome of the training process and the evaluation of the three most effective random forest regressions for minimising the height deviations between the  $ALS_{REF}$  and the  $IM_{ADJ}$  model can be found. The last section of the results, Chapter 4.3 concludes the results section by presenting the validation outcomes of the most effective random forest regression. This analysis aims to minimise height deviations between both models, providing results for evaluating the overall effectiveness and reliability of the chosen regression model.

# 4.1 Topographic products

In the following part of this thesis, the results of the derived topographic products such as the nDSM and the fractional cover and canopy mask will be presented. These products serve as the fundamental basis for the later performed training and test process of the random forest regression. The statistics calculated on basis of the nDSMs created here also serve as the input date for the validation process.

## Normalised digital surface models

The primary result of this study, and the basis for all further steps, is the normalised digital surface model (nDSM) presented in Figure 7. This representation of normalised land cover heights generates two distinct output files corresponding to the two acquisition methods. Although both data sets were acquired at comparable times, the deviations shown in Figure 8 between the nDSM from the IM data set (Figure 7(a)) and the normalised DSM from the ALS data acquisition (ALS<sub>REF</sub>) shown in Figure 7(b) can be seen. The normalised height models of the training area were scaled between -1 m and 60 m in relation to the underlying DTM from dark to light colours.

The major visual difference, which can even be observed without further analysis, is located in the south-eastern part of the training nDSM shown in Figure 7. In Figure 7(a), thinnings within the closed canopy can be identified in this zone. These are pixels of low normalised height values arranged in lines where trees were systematically removed. These areas are not adequately mapped when using the image matching process. Only from a certain size upwards, it is possible to successfully visualise these thinnings using the pixel based matching process from the aerial images within this dataset.

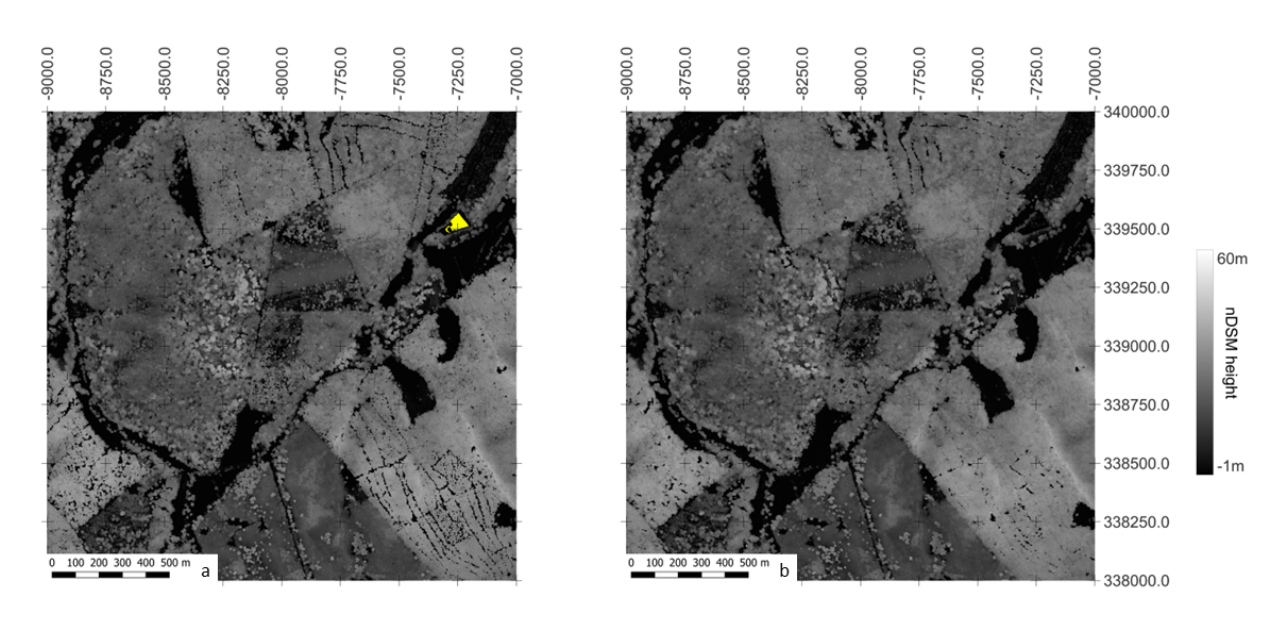


Figure 7: Representation of the normalised surface models (nDSM) for the training area in the region of the Lainzer Tiergarten around Johannser Kogel.

**Left:** (a) Visualisation of the nDSM generated by airborne laser scanning. The area in which no data could be acquired is highlighted in yellow.

**Right:** (b) nDSM from the image matching point cloud data.



In particular, low areas such as gaps within the closed canopy derived from the  $ALS_{REF}$ data, are not adequately represented in the IM nDSM. As can be seen in the difference image in Figure 8, these areas show a relatively high deviation between the two models. Within the difference raster image, those areas are shown as positive (red) in which the height of the IM data lies above the  $ALS_{REF}$  model which is assumed to be the reference. In contrast, blue areas within the figure indicate areas in which the normalised height values of the IM are below those of the  $ALS_{REF}$  nDSM. In the closed canopy, the IM heights tend to be lower than those from the ALS model. There are also larger deviations at the edges of the forest between the two acquisition methods.

As illustrated in Figure 7(a) and Figure 8, yellow coloured areas are marked in the northeastern part of the training area. These areas are indication pixels, where no data was acquired. According to a comparison of the orthophoto and the Geodatenviewer of the City of Vienna, the Grünauer Teich (Grünauer pond), an anthropogenically developed water body, is located in this area.

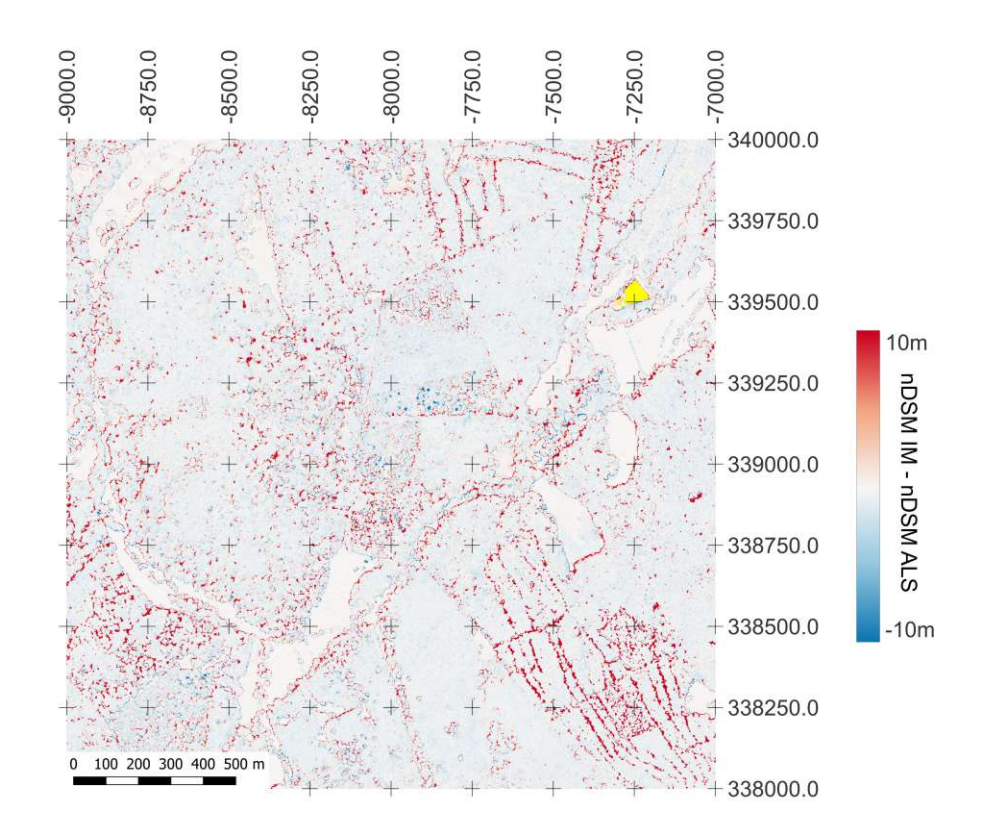


Figure 8: Illustration of the difference map between the nDSM obtained from ALS and IM, where the ALS, serves as reference value. Negative values indicate a lower elevation of the IM model while positive values indicate a higher IM model. The area in which no data could be acquired is highlighted in yellow.

### Fractional cover

In this thesis, the fractional cover is used to define overshadowed areas in forest areas. It is used to define the area that is considered to have high vegetation cover for the random forest regression.

The difference observed in the previous chapter within the closed canopy is also evident when comparing the fractional cover. When comparing the two areas covered by canopy (minimum over 90%), it can be seen that the area derived from the IM data is larger than the area derived from the  $ALS_{REF}$  model. The canopy area determined from the  $ALS_{REF}$  nDSM equals 3.21 km<sup>2</sup>, which is 0.17 km<sup>2</sup> less than the 3.38 km<sup>2</sup> obtained from

the IM method. Assuming a total area of 4 km<sup>2</sup>, the degree of coverage counts 80% for the nDSM obtained from the  $ALS_{REF}$  data acquisition and 84% in the IM surface model. This fact shows that the  $ALS_{REF}$  data has a higher proportion of gaps and unshielded areas compared to the IM data set.

# 4.2 Random forest regression

In the following chapter, the results of the modelling of the height differences of ALS and IM data based on features derived from IM nDSM in forest areas are presented.

The results of the random forest model for the approximation of the IM canopy height to the ALS canopy height are presented below. As described before in *Chapter 3.4*, hyperparameter tuning plays an important role when using machine learning and especially in the field of random forests. In the following two chapters, the hyperparameters: maximum depth and maximum number of estimators in the training process are described in more detail based on the results from the test process, carried out in the therefore defined areas. A variation of the input data, such as different kernel sizes for calculating statistical input parameters were also tested.

### 4.2.1 Kernel sizes / maximum depth

Figure 9 illustrates the performance assessment of the trained random forest regression model in terms of the height differences between the adjusted nDSM from the IM data  $(IM_{ADJ})$  and the given ALS nDSM  $(ALS_{REF})$  that represents the ground truth. For evaluation, a heatmap was created presenting different models of the random forest regression algorithm in terms of maximum depths and different kernel sizes used for calculating the statistics. The Root Mean Square Error (RMSE), median and Pearson's Correlation Coefficient (Pearson's R) for the height differences between the adjusted IM nDSM and the given nDSM are given in Figure 9(a-c)

As depicted in Figure 9(a), it is noticeable that the RMSE tends to rise as the kernel size of the input statistics increases. This indicates that larger kernel sizes decrease the prediction accuracy of the model. The highest RMSE value of 3.671 m occurs while using a kernel size of 7 (corresponding to an area of 15 by 15 pixels when calculating statistical parameters of a single pixel) while applying a maximum depth of 50. In contrast, the lowest RMSE and therefore the best result of 3.517 m occurs at a kernel size of 1 (corresponding to an area of 3 by 3 pixels during the moving window statistics calculation) and a maximum depth of 10.

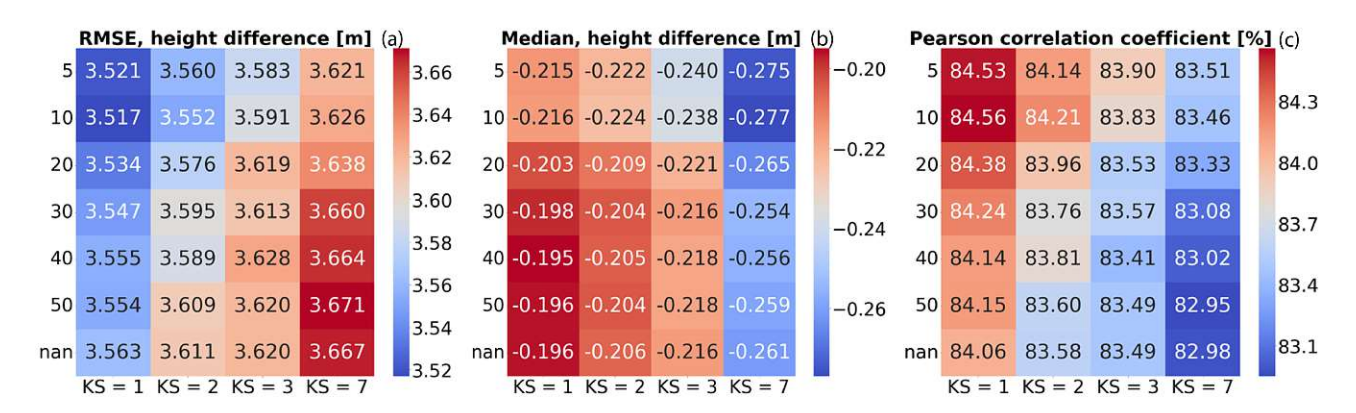


Figure 9: Results of the statistical parameters RMSE (a), median (b) and Pearson's R (c) as a function of the kernel sizes used to calculate the statistical input parameters (horizontal) and the maximum training depth (vertical) for a fixed number of estimators of 10 within the canopy mask.

The median value (Figure 9(b)) regarding the height deviation between the adjusted height model out of the IM data and the ALS ground truth  $(ALS_{REF})$  shows a similar pattern to the behaviour observable in the root mean square error, RMSE. As the kernel size increases, the median value also tends to increase. This trend in the median value culminates in a maximum negative value of -0.277 m when using kernel size 7. The minimum drops to a value of -0.195 m for a configuration between a maximum depth of TU **Bibliothek**, Die approbierte gedruckte Originalversion dieser Diplomarbeit ist an der TU Wien Bibliothek verfügbar wien knowledge hub. The approved original version of this thesis is available in print at TU Wien Bibliothek.

the training algorithm of 40 and a kernel size of 1. Using the largest neighbourhood of the input statistics, the median also indicates the largest average value of the different depths in the training. For example, for kernel size 7, the average value of the median is around -0.26 m, while the median, which is robust to outliers, has an average value of -0.2 m when using kernel size 1.

The analysis of the third evaluation parameter, illustrated in Figure 9(c) as the Pearson Correlation Coefficient which was 83.29% between the given IM and the given ALS, affirms the previous results. With an average correlation of 83.18%, kernel size 7 is generally below the average overall value of the parameters of 83.99%, while the average value for kernel size 1 is above average with a value of 84.24%.

As the kernel size increases, not only the previously described error values increase, the correlation decreases. A particularly high Pearson's R value is achieved at a depth of 10 and the smallest kernel size of 1 with 84.56%. The strongest correlation between the given ALS height model and the adjusted IM nDSM,  $IM_{ADJ}$  occurs in configurations that also have low values for the other error parameters. It must be said that such marginal differences of one percentage point are minimal and do not yield a significant difference.

### 4.2.2 Testing: Number of Estimators / maximum depth

Figure 10(a-c) shows the performance characteristics of the random forest regression, adjusting the maximum depth and number of estimators used for training the regression model. The parameters RMSE, median and Pearson's R were used to evaluate the success of the training procedure.



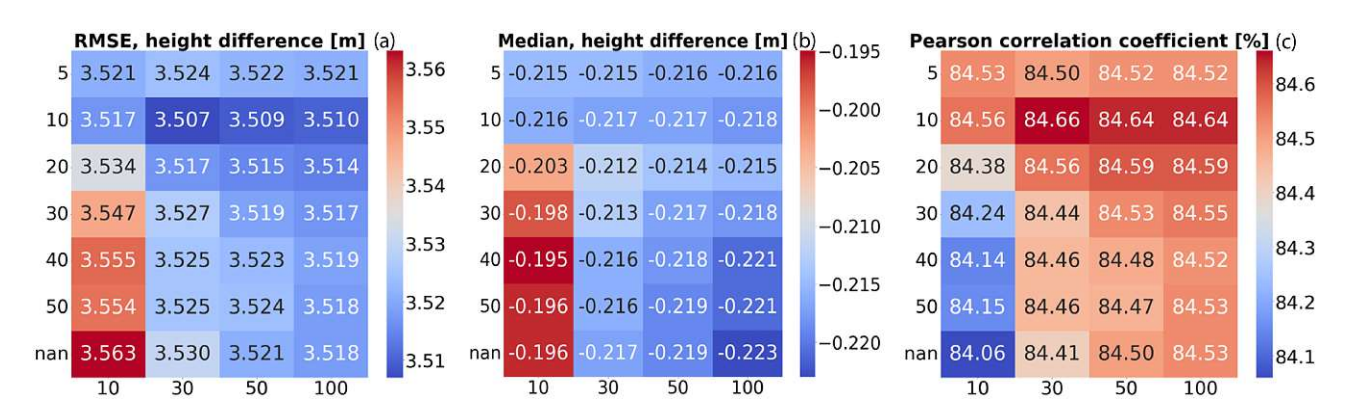


Figure 10: Illustration of the statistical parameters RMSE (a), median (b) and Pearson's R (c) of the difference between the adjusted nDSM out of the IM data and the given reference ALS nDSM in a heatmap for evaluating results of different numbers of estimators (columns) at different maximum depths of training (rows).

When looking at the different depths, it can be observed that a maximum depth of ten during the training process provides the lowest RMSE value of this test series. Here a RMSE of 3.507 m was reached while using 30 estimators, which is clearly below the average overall RMSE value of 3.526 m. In general, a maximum depth of ten nodes across the different numbers of estimators gives the lowest average RMSE value of 3.509 m. In the row representing the values of the RMSE at unlimited depth, a clear decrease in accuracy can be observed. In this case, the average value for the class of unlimited depth regarding the RMSE over all estimators increases up to a maximum of 3.563 m with an average value of 3.533 m. A maximum depth of 30 nodes results in an average RMSE value of 3.527 m. The heatmap in Figure 10 also shows that a higher number of estimators in combination with lower depths also show slightly lower deviations, whereas a deeper process in the training brings an increase in the RMSE value.

In the analysis of Figure 10(b), it can clearly be observed that the accuracy increases and reaches the lowest median value of -0.195 m at a depth of 40 nodes and a number of ten estimators, the minimum in this series of tests, while the maximum is -0.223 m and occurs in the test series for unlimited depth in the training. The column that draws the results

over different depths by using ten estimators in the training process of the random forest regression, again gives the best average result of the median as before. As the number of estimators increases, the value of the mean height difference in relation to the median between the adjusted IM and the ground truth  $ALS_{REF}$  also increases. The average value for all depths is -0.202 m with ten estimators and increases to -0.219 m while applying 100 estimators.

The third and last parameter, shown in Figure 10(c), is the relationship between the adjusted IM and the ground truth ALS model. The Pearson Correlation Coefficient consistently exceeds 84% across all configurations employed during training. This indicates a strong correlation within the data across all variants. The average overall Pearson's R is 84.48% while the maximum, at 30 estimators and a depth of ten, has a value of 84.66%. The minimum of 84.06% at unlimited depth of training and ten estimators is still above the average value of 83.99% presented in the previous heatmap in Figure 9(c) for the different input kernel sizes.

Based on the heatmaps described above, those three regression models were selected for further analysis that were able to achieve a global minimum across all models within the training process.

Tab. 3: Summary of the statistical results of hyper parameter tuning in the training process for the three best random forest regression models in terms of mean, median and RMSE of the deviations between the adjusted model and the ground truth.

CONFIG	$0710\_1307$	$2310_{-}2228$	$2310_{-}2320$
Kernel size	1	1	1
Nr. of estimators	10	30	30
$Max \ depth$	40	10	None
Mean [m]	0.278	0.302	0.275
Median [m]	-0.195	-0.217	-0.217
Std. deviation [m]	3.545	3.494	3.519
RMSE [m]	3.555	3.507	3.530
Pearson's R [%]	84.14	84.66	84.41



On one hand, Table 3 enumerates the input data used as the kernel size of the statistical input files, the number of estimators used and the maximum depth of the training process in the random forest machine learning process. On the other hand, the statistical evaluations of the three best configurations are displayed as a summary. Within the statistical evaluation of the height differences between the adjusted  $IM_{ADJ}$  and given ALS nDSM in the forested area, the mean, median, standard deviation and RMSE are used for the configurations listed in Table 3. The individual minima of the evaluation criteria over all tested configurations (n = 70) are marked thickly in the table. The configuration 0710\_1307 (representing date and time of training) achieves the lowest result of the median related to the height differences between the adjusted IM nDSM and the given ground truth  $ALS_{REF}$ . To achieve the lowest value of differences with respect to the RMSE, configuration 2310\_2228 must be used. Configuration 2310\_2320 shows the lowest value of the median of height deviations among the total of 70 trained values regression models.

### 4.2.3 Minimum median regression

In the following section, the results of the median minimising random forest regression will be presented. The analysis is based on the following aspects: individual tree heights, the canopy structure based on a test strip in the area investigated and the distribution of the height deviations between the  $IM_{ADJ}$  and the  $ALS_{REF}$ .

### Single tree heights

Figure 11 shows the single tree heights in the area for testing the random forest regression as Boxplots.

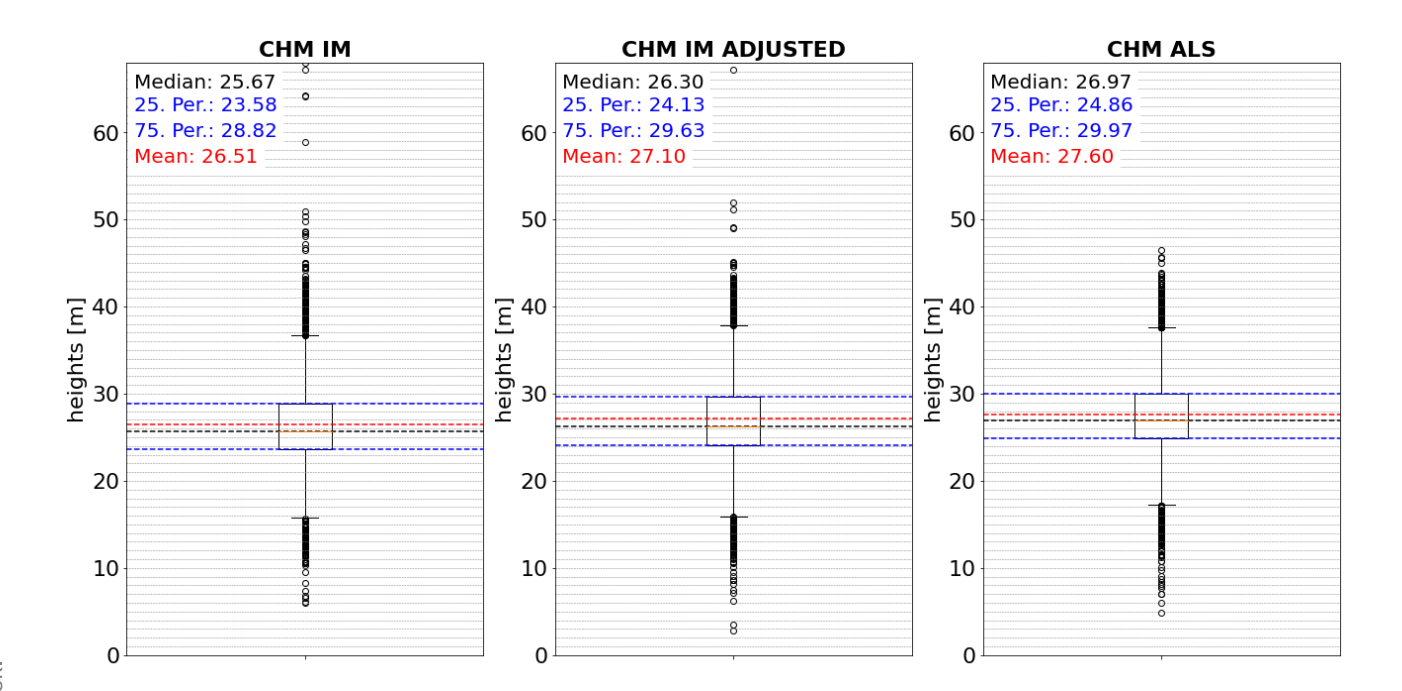


Figure 11: Representation of the heights of selected individual trees within the training area as a boxplot for trees from the IM, adjusted IM and ALS data. The median (black), quantiles (blue) and the mean values (red) are shown for each dataset as dashed lines. The model used for this Figure was the median minimizing regression.

The positions of the height measurements were determined using the "ForTreeDetection" tool implemented in OPALS (please refer to OPALS, n.d.-a). Statistical parameters for quantiles are marked as dashed lines in blue in the three boxplots, as well as the median, which is robust against outliers in black and the mean value in red.

The median of the single tree heights from the IM CHM, 25.67 m, tends to be lower than the corresponding value from the ALS shown in Figure 11, which is assumed as the ground truth. The median height of the individual trees found within the ALS canopy mask is 26.97 m above ground. After applying the random forest regression to the IM data set, the average mean height of individual trees could be adapted to 26.30 m in the  $IM_{ADJ}$  model, which is an improvement of the differences regarding the median value of 48.5% compared to the original deviation between the IM and the ALS median height. After the execution of the regression model, the median difference between the average

adjusted single tree heights and the average single tree height of the groundtruth of 1.3 m could thus be improved by 0.63 m to 0.67 m between the ALS heights and the adjusted IM heights.

Despite the existing outliers in the IM, which were not removed by the filtering process of BFW, the outlier sensitive mean is below the  $ALS_{REF}$  mean value for the individual trees within the canopy mask. At 27.06 m the mean  $ALS_{REF}$  single tree height above ground is 1.09 m higher than the mean value from the CHM of the IM surface model. By applying the regression function, this difference could be reduced by about 54% and raised to a mean value of 27.10 m in the  $IM_{ADJ}$ , which also represents a significant approximation of the IM model.

## Canopy height Model

Figure 12 represents a cross section canopy heights generated from the two (ALS<sub>REF</sub> and IM) respectively three (also  $IM_{ADJ}$ ) different acquisition methods. The profile shown in Figure 12 represents a 1 pixel wide (1 pixel = 1 m) strip with a length of 400 m.

Illustrated in Figure 12, the elevation values in the IM CHM are approximated in comparison to the normalised  $ALS_{REF}$  elevation (depicted in black), which is used as reference. The canopy height plot (CHP) also illustrates peaks within the  $IM_{ADJ}$  nDSM which are evidently lower in elevation than the input elevation provided for the IM. Although the  $ALS_{REF}$  is above the IM at these specific locations as anticipated, the regression clearly predicted a considerably inaccurate value. Furthermore, it can be observed that the heights of the CHM derived from the IM data tend to have a lower variability with respect to their canopy surface than the height values derived from the  $ALS_{REF}$  height model.

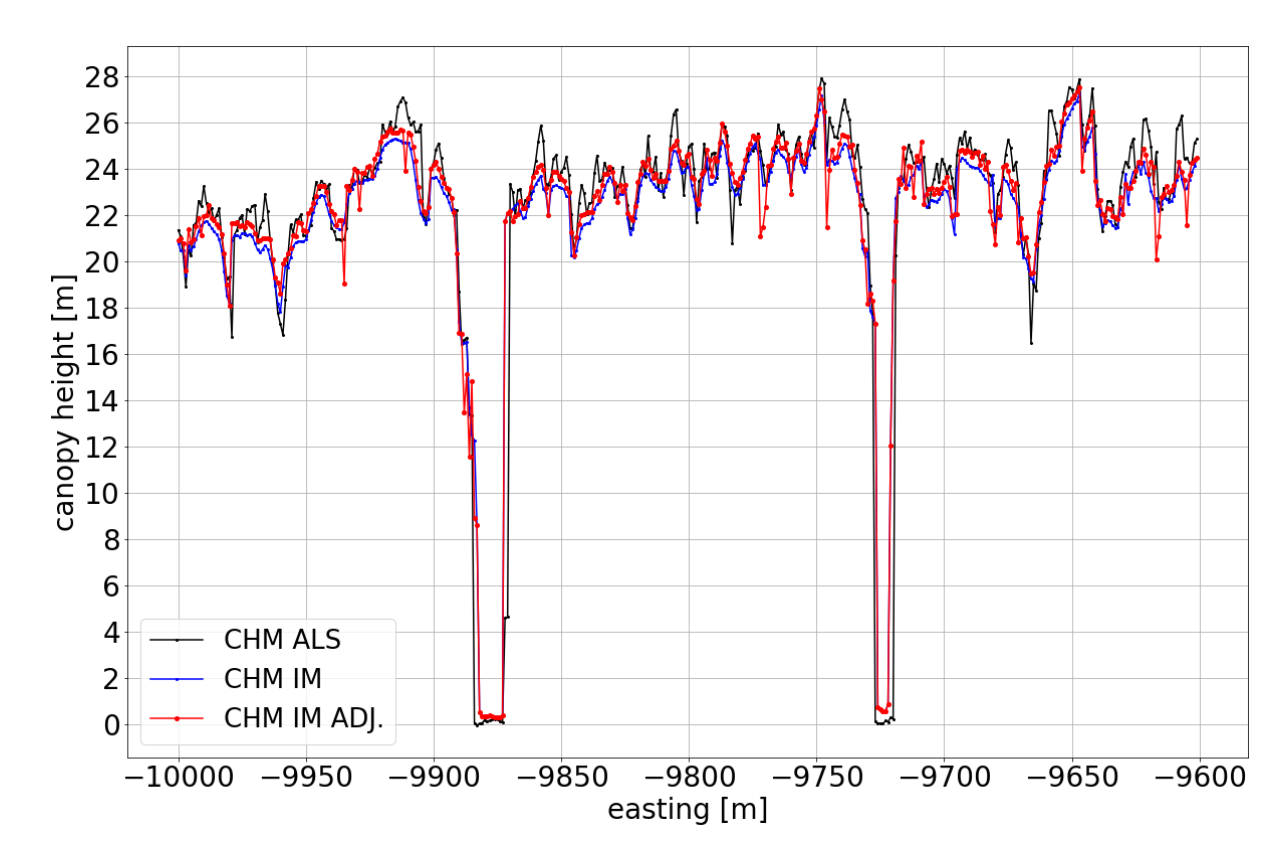


Figure 12: Visualisation of a 400 pixel by 1 pixel (1 m = 1 pixel) wide test strip in which the height values were extracted from the CHM. The reference model from the ALS acquisition method is shown in black. Blue indicates the original canopy shape from the IM data and red visualises the improved median minimising random forest model approximated to the ALS.

In areas where the canopy cover falls below the threshold value of 90%, the adjusted canopy heights and the IM models match, as in these zones the developed algorithm integrates the height values directly from the available IM data. For example, in the gaps within the closed canopy, it can be observed that these gaps are narrower in relation to their representation width in the plot of the IM than the gaps from the ALS CHM. The normalised heights of the IM in the unshaded area of the forest also tend to be slightly higher than in the given ALS. However, this effect is exactly reversed in the canopied areas.

### Distribution of height differences

The histogram depicted in Figure 13 illustrates the disparities in height between the provided ALS height model and the adjusted model derived from the IM data which specifically focus in pixels within the created canopy mask.

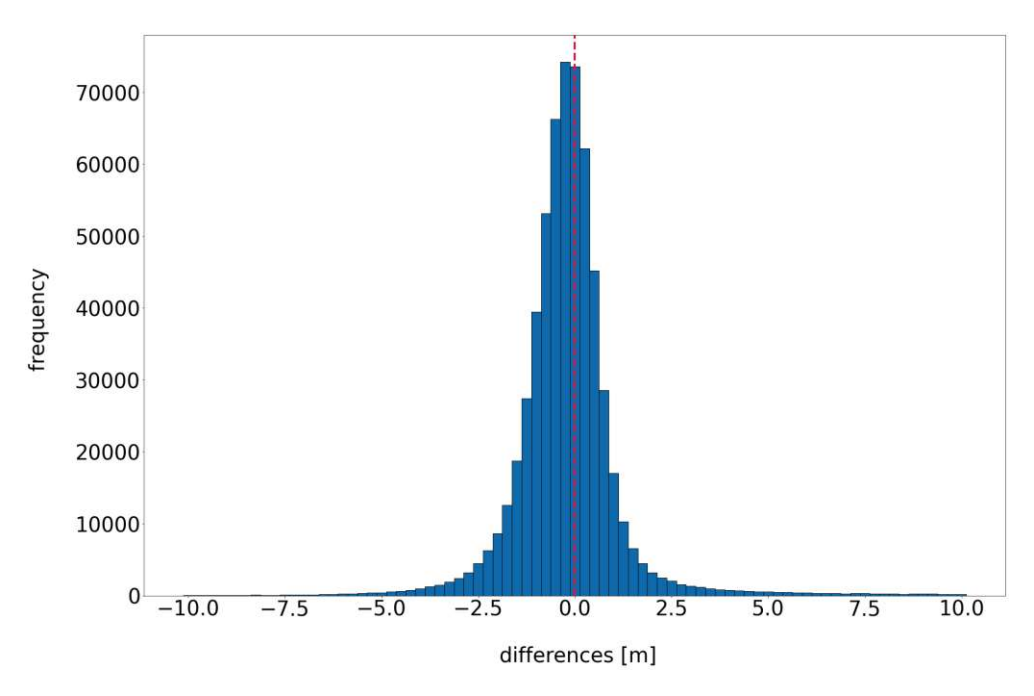


Figure 13: Histogram of the height deviations [m] between the ground truth and the adjusted canopy height values using a median minimising random forest regression. The red dashed line serves as a reference for 0 m deviation. The class width used is 0.25 m.

The height differences are presented in a range of  $\pm$  10 m, wherein a negative value indicates a pixel to be predicted too low compared to the ground truth and vice versa. The X-axis of the histogram describes the height differences in metres with a resolution of 0.25 m. The frequencies of the corresponding deviations are plotted on the Y-axis. The red dashed line represents the zero value, an identical model between  $ALS_{REF}$  and the  $IM_{ADJ}$ , with a deviation of  $\pm 0.125$  m.

With this configuration, the height difference distribution reveals an accumulation of the deviations around the value -0.25 m, which means 0.25 m below the ALS model. The

median of the deviations of the model in this case is at 0.195 m, signifying a minor predicted underestimation for the ALS reference model. Here, the minimum deviation is -29.76 m, indicating an excessive underestimation, while the maximum deviation is 63 m. This signifies an overestimation compared to the ground truth. The histogram shows that the adjusted model tends to be lower in the median than the  $ALS_{REF}$  model.

### 4.2.4 Minimum mean regression

### Single tree heights

The data shown in Figure 14 represents the height model derived from the random forest regression that delivered the lowest value for the mean value of the deviations between ground truth and prediction.

The mean value of the selected tree heights in the test area reached 27.0 m (0.1 m lower than in the previous model) with a median of 26.26 m, which is also slightly below the value of the previous model in *Chapter 4.2.3*. In this case, the average height difference in relation to the median from the tree heights of the  $ALS_{REF}$  which amounts 1.3 m was reduced by 45% to 0.71 m within the  $IM_{ADJ}$ . The difference in the mean was reduced from 1.09 m between the IM and the  $ALS_{REF}$  data, to 0.6 m in the adjusted IM. This equates to an improvement in deviation of about 45% when comparing the ground truth with the heights of the adjusted IM data. Compared to the model from *Chapter 4.2.3*, a reduction in the quantile range between the  $25^{th}$  and  $75^{th}$  quantile in the adjusted IM can be observed. This value decreased from 5.5 m in the previously described  $IM_{ADJ}$  model to a value of 5.27 m in the model described in this chapter.

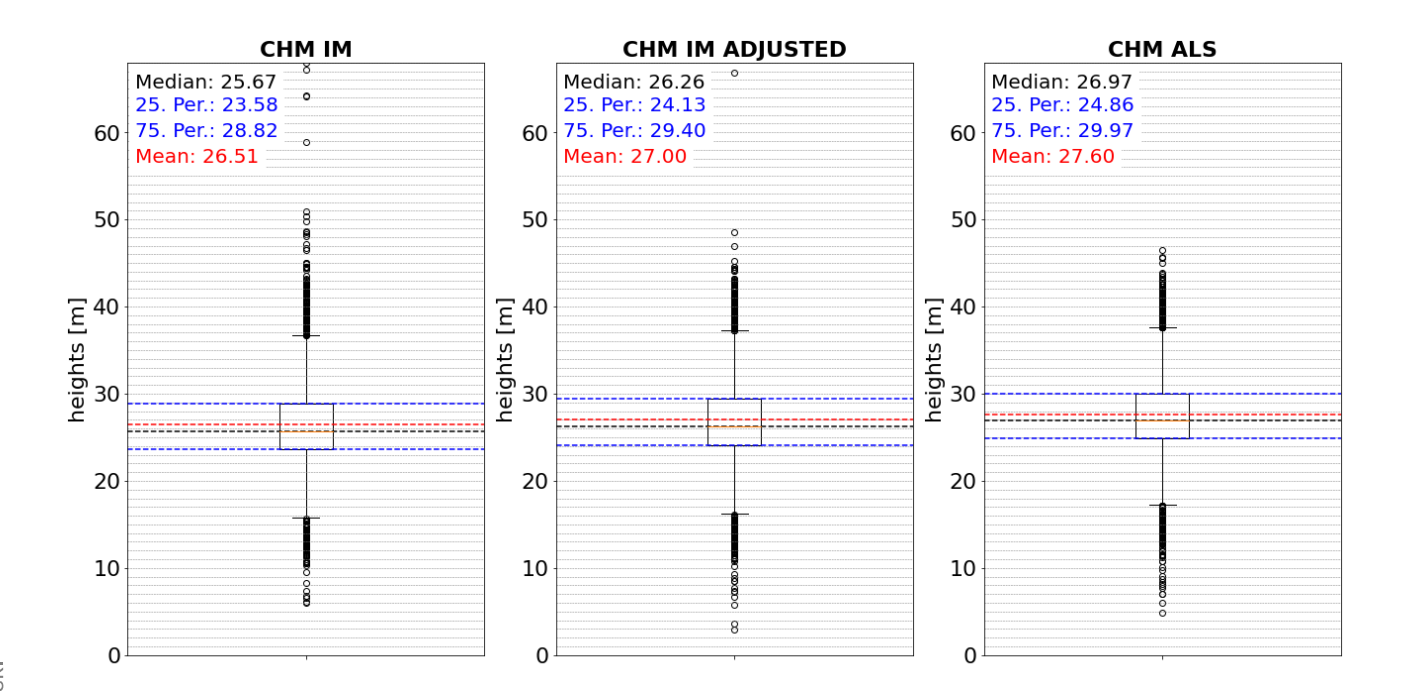


Figure 14: Representation of the heights of selected individual trees within the training area as a boxplot for trees from the IM, adjusted IM and ALS data. The median (black), quantiles (blue) and the mean values (red) are shown for each dataset as dashed lines. The model used for this Figure was the mean minimising regression

### Canopy height Model

The canopy height plot (CHP) shown in Figure 15 again represents the previously described area around the center coordinate -9800 m and 3337400 m in the test area. The values of the Y-axis once more represent the heights of each pixel along this line normalised by the DTM.

In contrast to the preceding model the CHP shows a more homogeneous pattern regarding potential outliers. In the selected part, there are fewer outliers in the direction of 0 m height above ground in the area of the closed canopy. In the part of forest gaps, a slight change in the height behaviour in the range between 14 m and 18 m above ground can be observed in comparison to the previous canopy height plot. Here, the edges tend to adapt to the given ground truth and again show less variability in height.

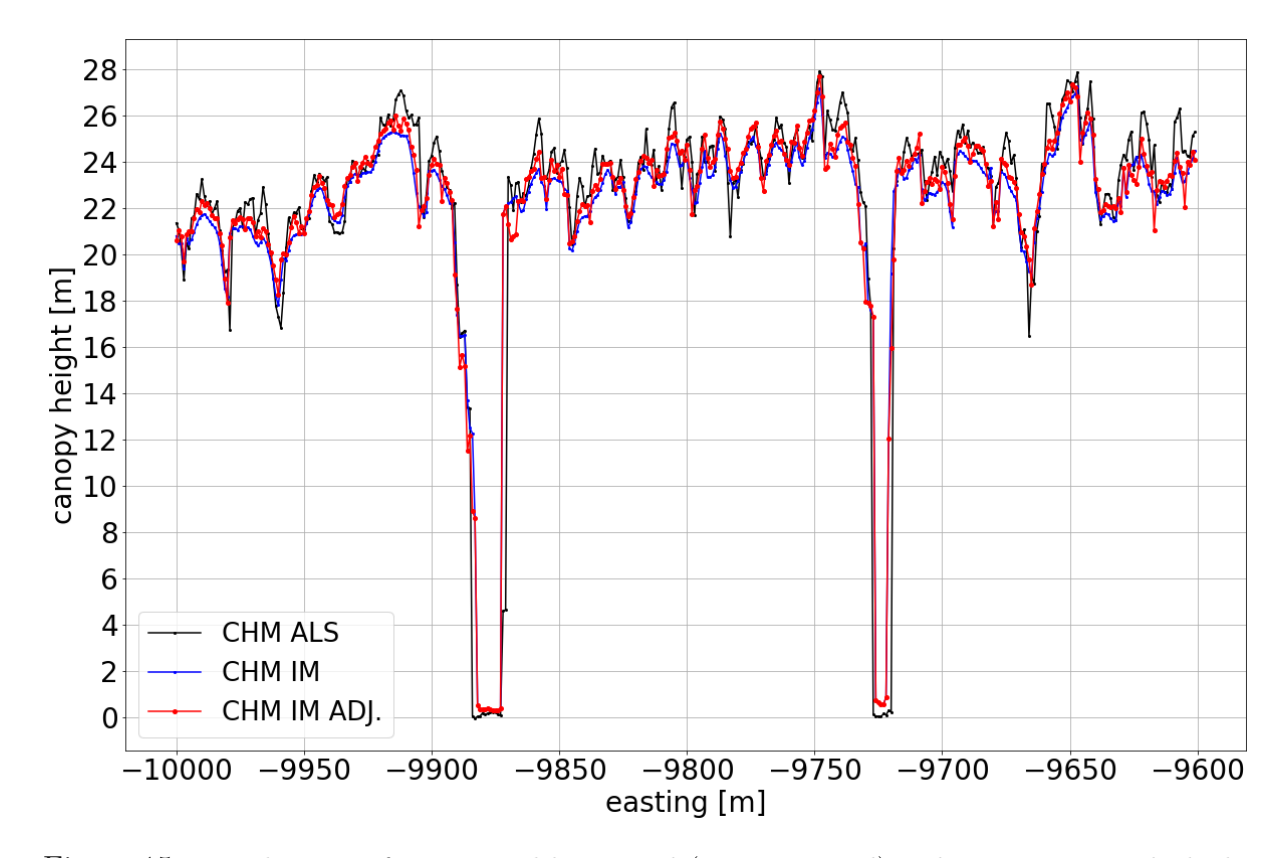


Figure 15: Visualisation of a 400 pixel by 1 pixel (1 m = 1 pixel) wide test strip in which the height values were extracted from the CHM. The reference model from the ALS acquisition method is shown in black. Blue indicates the original canopy shape from the IM data and red visualises the improved mean minimising random forest model approximated to the ALS.

### Distribution of height differences

The histogram of the height deviations between the ground truth and the adjusted model with the lowest value for the mean of the height differences is visualised in Figure 16. A slight increase in the cumulative value of 0.25 m compared to the histogram shown in Figure 13 can be observed in this diagram. In this model, both the minimum and maximum values, as well as the outliers, slightly increase. With an overestimation in the adjusted  $IM_{ADJ}$  a height difference of 65.69 m to the reference value and an underestimation of -35.28 m, the standard deviation decreases slightly to a value of 3.52 m.

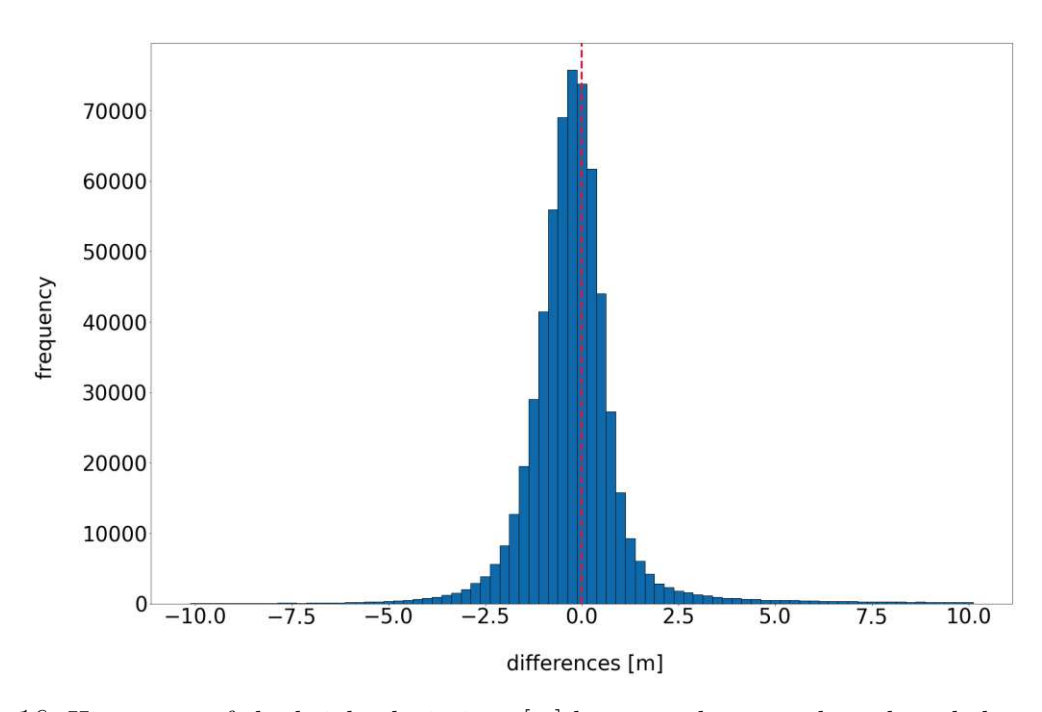


Figure 16: Histogram of the height deviations [m] between the ground truth and the adjusted IM canopy height values using a mean minimising random forest regression. The red dashed line serves as a reference for 0 m deviation. The class width used is 0.25 m.

## 4.2.5 Minimum RMSE regression

### Single tree heights

The result of the model that minimises the RMSE shows a similar trend in Figure 17 as the previously described methods. The span between the  $25^{th}$  and  $75^{th}$  quantile slightly decreased compared to the previous models and lies at 5.21 m (previously 5.5 m in the model of Chapter 4.2.3 and 5.27 m in the model explained in Chapter 4.2.4). The median of the detected single trees within the adjusted IM model has a value of 26.1 m above ground. This equals to a decrease of 0.2 m compared to median minimizing model and thus shows a deviation of 0.87 m (3.3%) below the reference model  $ALS_{REF}$ . Furthermore, one can also observe a decrease in the mean value when using the RMSE minimizing model, 26.85 m, which means a deviation of 0.75 m from the ground truth.

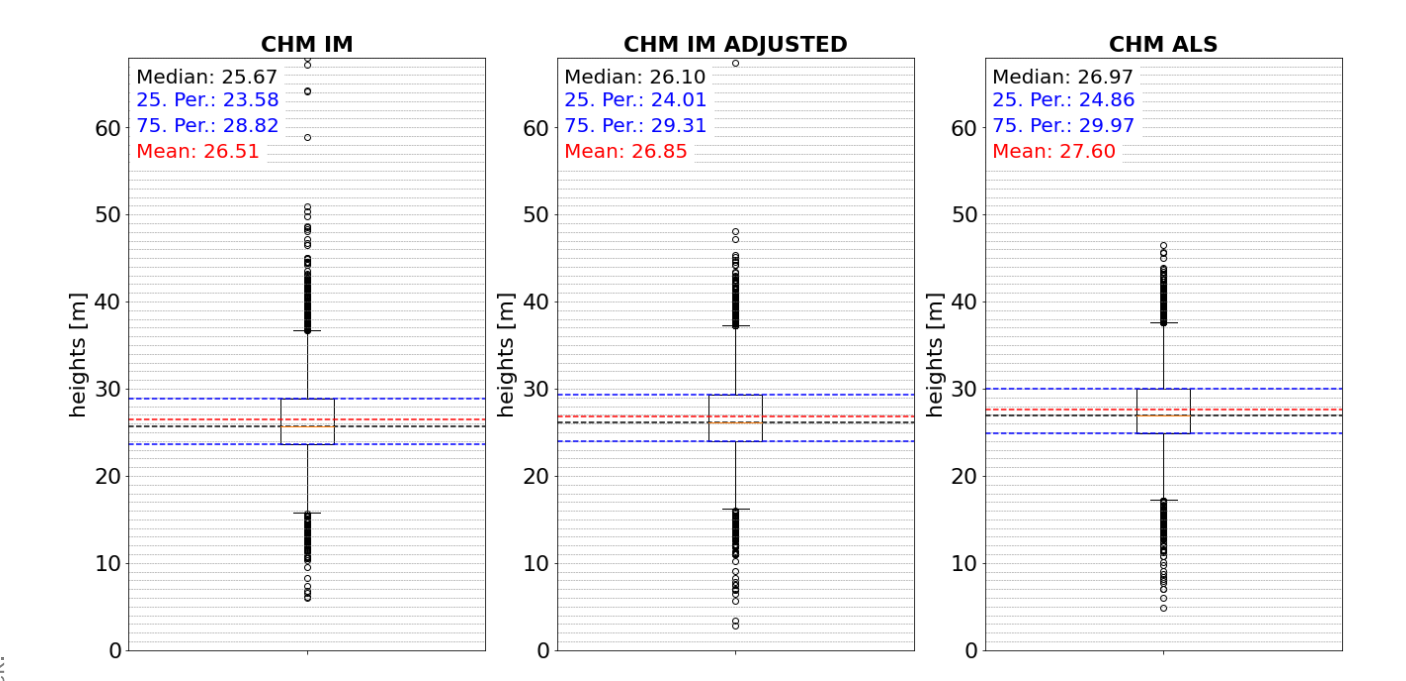


Figure 17: Representation of the heights of selected individual trees within the training area as a boxplot for trees from the IM, adjusted IM and ALS data. The median (black), quantiles (blue) and the mean values (red) are shown for each dataset as dashed lines. The model used for this Figure was the RMSE minimizing regression

### Canopy height Model

Figure 18 also shows the canopy height model in a cross section within the test area. For this calculation, the algorithm that minimised the RMSE was chosen to generate the data used for the displayed CHP. The model used in this chapter, has similar characteristics to the IM model highlighted in blue. The adjusted IM CHM shows only a few outliers in the direction of height 0 m. Areas that tend to have higher values compared to their neighbouring pixels in the ALS reference model are less adjusted by the RMSE minimizing regression than in the previous models. However, they show a general approximation of the height values within the closed canopy.

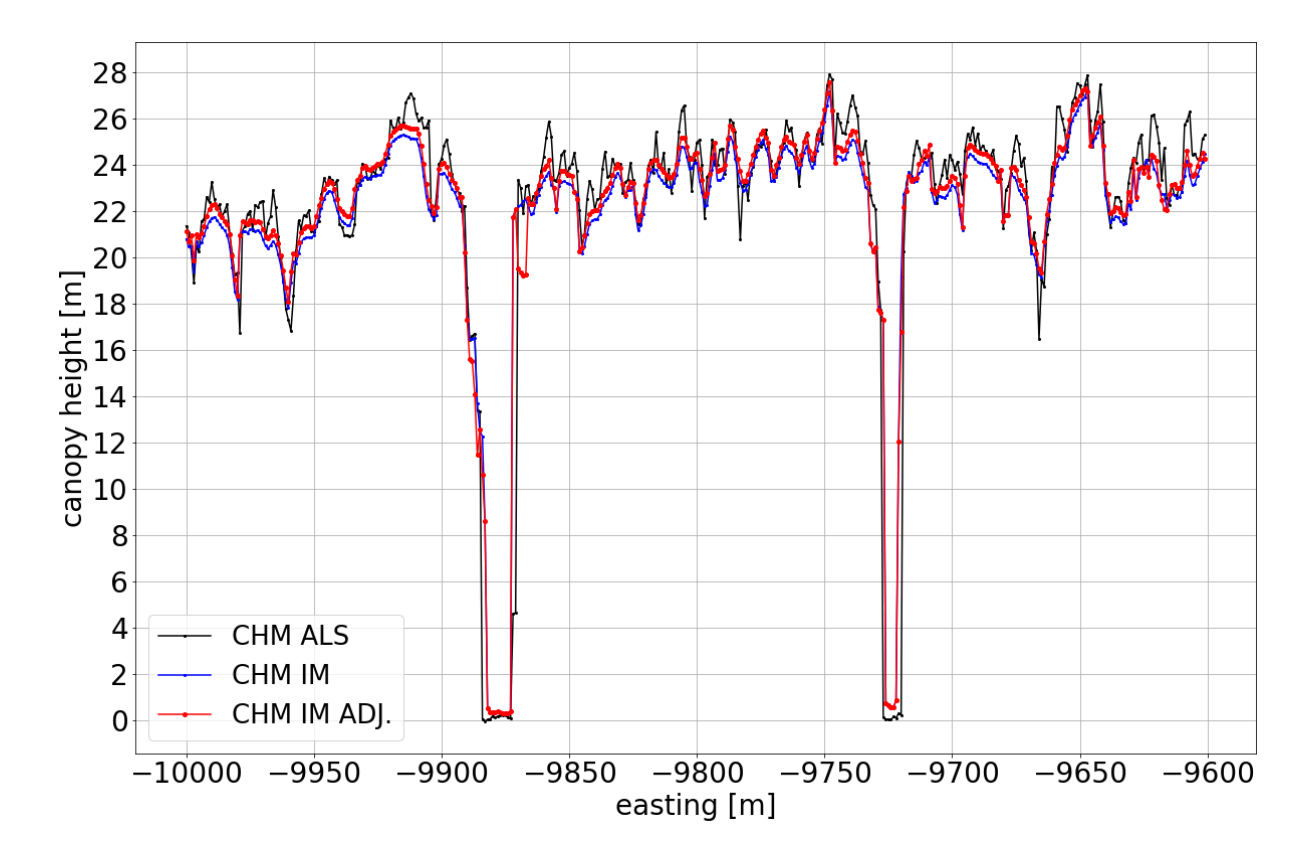


Figure 18: Visualisation of a 400 pixel by 1 pixel (1 m = 1 pixel) wide test strip in which the height values were extracted from the CHM. The reference model from the ALS acquisition method is shown in black. Blue indicates the original canopy shape from the IM data and red visualises the improved RMSE minimizing random forest model approximated to the ALS.

The behaviour in the areas of forest gaps provides similar properties as previously described. Especially in the area of the first gap (approximately at easting = -9925 m) it is noticeable that in the transitional zone between the gap and the forest, obvious differences in the height values occur compared to the other two tracks (input model and reference model). Both input models indicate heights of around 22 m, whereas the adjusted IM model shows a deviation of 3 m, reaching a value of 19 m in this area.

### Distribution of height differences

Figure 19 illustrates the histogram of the frequencies of deviations between the adjusted IM and the given ALS data set. In this part, the RMSE minimizing regression model was applied on the IM nDSM. An increase of the cumulation by the value of zero and -0.25 m can be observed. The standard deviation as well as the RMSE are lower compared to the other two previously described models with a value of 3.49 m standard deviation and 3.51 m RMSE. The largest overestimation in this model is around 67 m above the ALS model and the smallest underestimation within the  $IM_{ADJ}$  CHM compared to the reference CHM amounts -31.6 m.

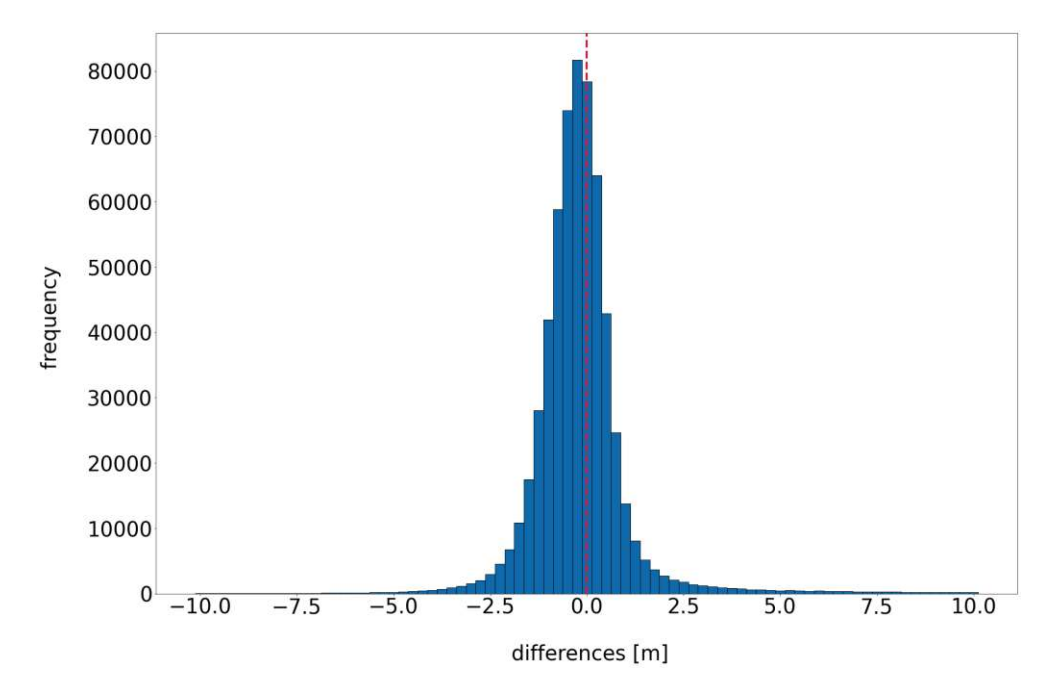


Figure 19: Histogram of the height deviations [m] between the ground truth and the adjusted canopy height values using a RMSE minimising random forest regression. The red dashed line serves as a reference for 0 m deviation. The class width used is 0.25 m.

# 4.3 Validation results

In Chapter 4.2, the optimised configuration of the random forest regression model was determined. The validation and accuracy assessment of the model will be presented in the following section.

### 4.3.1 Validation: Area 1

The results of the first validation area are visualised in the following histogram, Figure 20. It shows a normal distribution of the deviations from the reference CHM around the value of zero. A deviation of zero in this case indicates a deviation between  $\pm 0.125$  m between the  $ALS_{REF}$  and the adjusted CHM  $IM_{ADJ}$ .

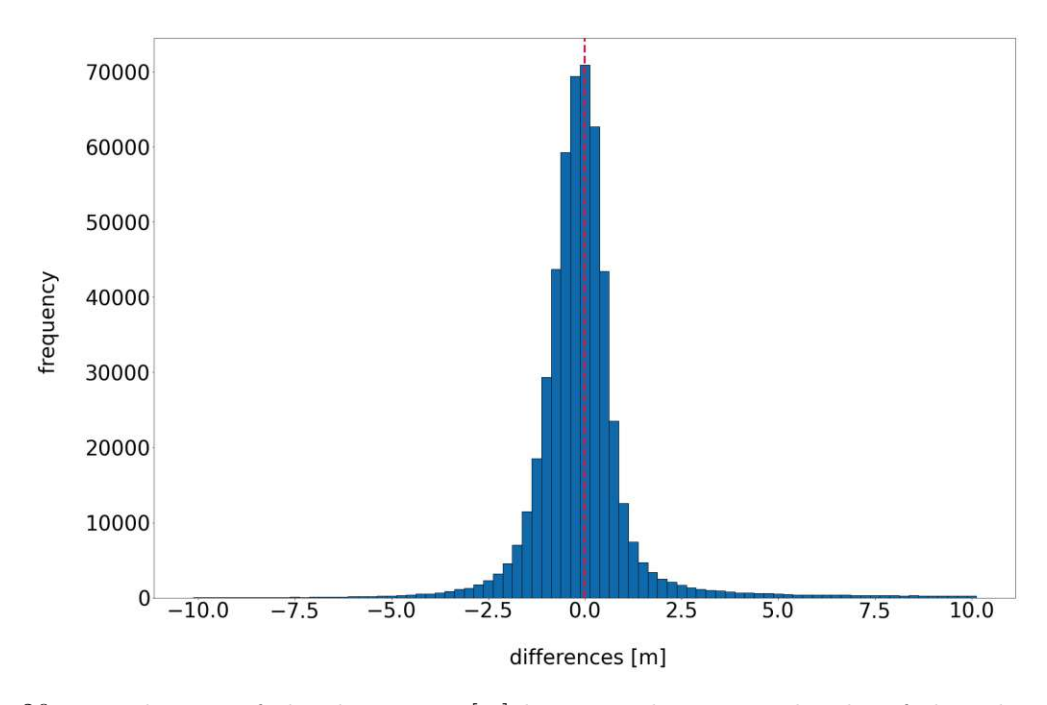


Figure 20: Distribution of the deviations [m] between the canopy height of the adjusted IM model and the reference model on a histogram in the scale range -10 to 10 m with a class width of 0.25 m. The red line indicates a deviation of 0 m from the ground truth within validation area 1.

A tendentious underestimation of the model is shown with a median value of -0.09 m whereas the outlier sensitive mean reaches a value of 1.18 m. The minimum value within this prediction of the heights in the canopy mask amounts an underestimation of -30.42 m compared to the reference CHM of the  $ALS_{REF}$  dataset. Within the adjusted IM CHM the absolute maximum of the deviation is 57.64 m above the reference model, leading to a span of 88.06 m between the highest and lowest pixel in the prediction. The RMSE of the validation process in the first area attains a value of 5.92 m, as depicted in Table 4. This table indicates the values for the median, mean and RMSE of the differences between the IM data and the reference ALS CHM. Furthermore, those values are also calculated for the difference between the adjusted  $IM_{ADJ}$  and the ground truth  $ALS_{REF}$  in meters. The adjustments are also indicated in this table and it can be seen that the median and the RMSE could be improved compared to the difference between the original IM canopy heights and the ALS canopy heights. Only for the mean, there was a slight increase of 0.24 m due to outliers. The median was reduced by 0.39 m and the reduction of the RMSE of the height difference was 0.19 m.

Tab. 4: Statistical characteristics of the differences between ground truth and the adjusted IM model in validation area 1. The adjustments compared to the original difference between the given IM CHM and the  $ALS_{REF}$  CHM are shown in the lower part of the table for the values mean, median and RMSE.

Deviation between $IM_{ADJ}$ & ALS			Deviation between IM & ALS			
	$\mathbf{Mean}_{ADJ}$	$\mathbf{Median}_{ADJ}$	$\mathbf{RMSE}_{ADJ}$	$Mean_{REF}$	$Median_{REF}$	$RMSE_{REF}$
	1.18 m	- 0.09 m	$5.92 \mathrm{m}$	0.94 m	- 0.48 m	6.11 m
	Adjustment					
	+ 0.24 m	+ 0.39  m	- 0.19 m			

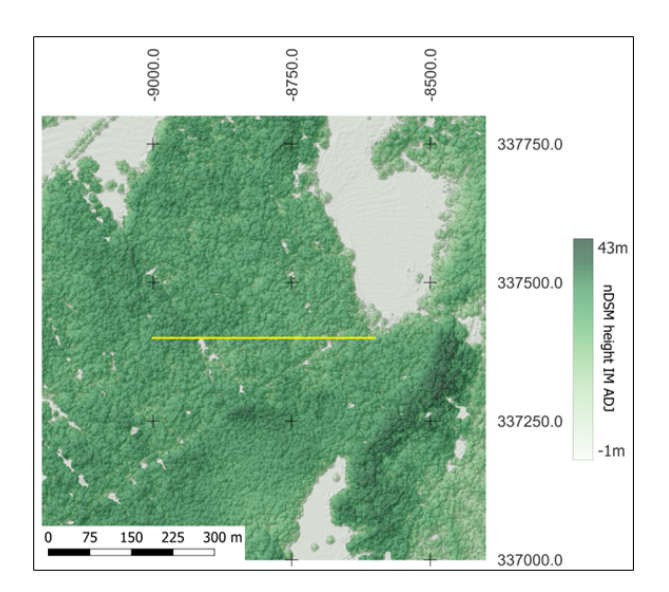


TU **Sibliothek**, Die approbierte gedruckte Originalversion dieser Diplomarbeit ist an der TU Wien Bibliothek verfügbar wien vour knowledge hub

The approved original version of this thesis is available in print at TU Wien Bibliothek.

To illustrate the numerical parameters represented earlier in Table 4 and the histograms from Figure 20, Figure 21(a) visualise the adjusted IM elevation model in a range of -1 m to 43 m normlised with the DTM from *Chapter 2.3.4*. In this area, the normalised surface respectively canopy height is shown in different shades of green from low (light green) to high (dark green).

The difference plot shown in Figure 21(b) represents the deviations of the adjusted IM model to the reference model. To improve the visualisation of these difference values, they were scaled in a range of -10 m to +10 m. All areas highlighted in red indicate areas which were predicted too high. In other words, areas in which the adjusted IM nDSM  $(IM_{ADJ})$  is higher than the reference value in the  $ALS_{REF}$  nDSM. The brighter the area in the image, the closer the prediction is to the reference value and the deviation is close to zero. Blue areas indicate an underestimation of the normalised height, where the adjusted IM CHM is under the value assumed to be true from the  $ALS_{REF}$ . All areas outside the canopy mask created in *Chapter 3.3.1* are not included in the difference model generation. They are shown as grey areas in this visualisation, as they were taken directly from the input nDSM and no improvement has been applied yet.



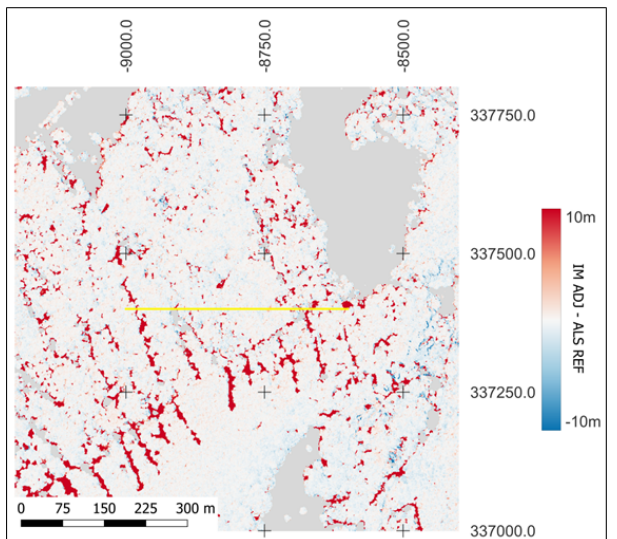


Figure 21: Left: (a) Illustration of the adjusted normalised elevation model in validation area 1, between -1 m (light) and 43 m (dark). **Right:** (b) Representation of the difference image between the reference ALS and the IM nDSM adjusted. In both plots, the yellow line shows the investigation area for the canopy height plot.

The yellow line displayed in the adjusted IM nDSM as well as in the difference model visualised in Figure 21 represents the area used for the comparison and visualisation of the canopy height using the CHP. Again, a 1 by 400 pixel area (1 pixel equals 1 m) was selected from the centre of the validation area. The pixel values of this section were plotted as a function of their height per pixel in the three different models (IM nDSM, ALS nDSM (ALS<sub>REF</sub>) and adjusted  $IM_{ADJ}$ ).

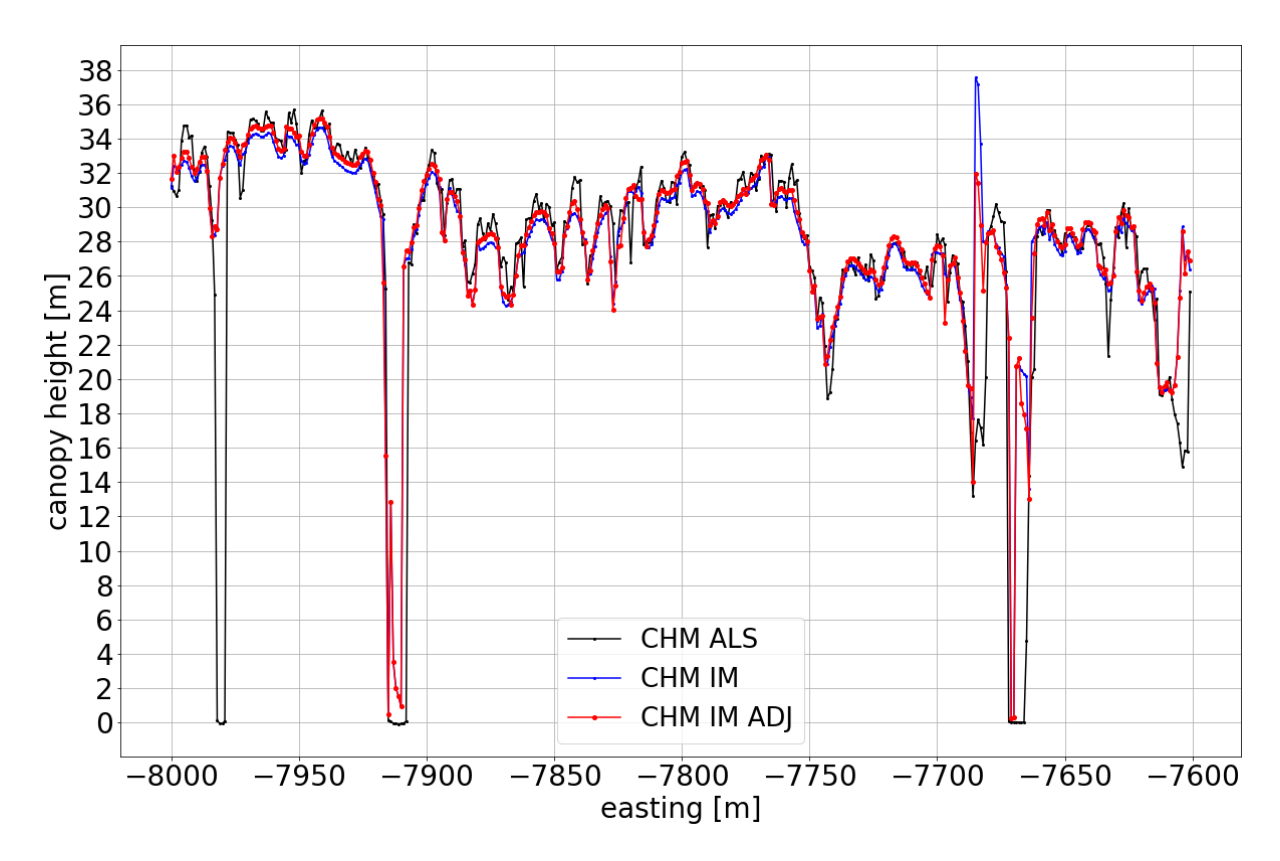


Figure 22: Presentation of the canopy height plot within the selected strip in validation area 1. ALS nDSM heights are shown in black and the input values of the IM nDSM in blue. The adjusted IM values  $(IM_{ADJ})$  are shown as red in the plot.

In Figure 22, an improvement and approximation of the height values from the adjusted IM dataset to the ground truth is shown, whereby the adjusted values  $IM_{ADJ}$  do not completely correspond to the strongly varying ALS canopy. It can be observed that the properties of the  $IM_{ADJ}$  are more similar to the original IM data. The improvement is particularly noticeable in the outliers of the IM dataset and in the approximation for those pixels.

Both the canopy height plot for the test strip and the difference plot show that the prediction for values recognised in the  $ALS_{REF}$  as forest aisles or as smaller clearings within the closed canopy can only be predicted with difficulty from the given IM nDSM.

# TU **Sibliothek**, Die approbierte gedruckte Originalversion dieser Diplomarbeit ist an der TU Wien Bibliothek verfügbar wien vour knowledge hub The approved original version of this thesis is available in print at TU Wien Bibliothek.

### 4.3.2 Validation: Area 2

The histogram in Figure 23 for the second validation area also shows a normal distribution and has the highest accumulation of deviations from the reference model around the value zero. For this area, the maximum overestimation is 47.57 m while the minimum deviation from the reference nDSM  $ALS_{REF}$  is -21.96 m below the actual value. Upon inspection of the histogram, a subtle underestimation of the model compared to the reference becomes apparent, with a median error of -0.09 m.

The difference plot (Figure 24(b)) presents a more homogeneous pattern with less significant deviations and fewer dark red areas compared to visualisation of the previous model in Figure 21. As in the previous area, the deviations are shown in a range of values between  $\pm$  10 m from red to blue. The adjusted IM nDSM in Figure 24(a) is visualised in a range of -1m to 30m below and above the DTM.

The average value (mean) of the deviations after applying random forest regression is 0.14m, as shown in Table 5. The original deviation between IM and  $ALS_{REF}$  was -0.23 m, indicating a transition from an average underestimation to an overestimation with respect to the mean value. According to Table 5, the RMSE could be reduced from its original value of 2.14 m to 2.07 m, representing a reduction of 0.07 m. The median, improved from -0.5 m to -0.09 m in the difference between  $ALS_{REF}$  and the adjusted IM, shows an improvement of 82% compared to the difference between IM and ALS.

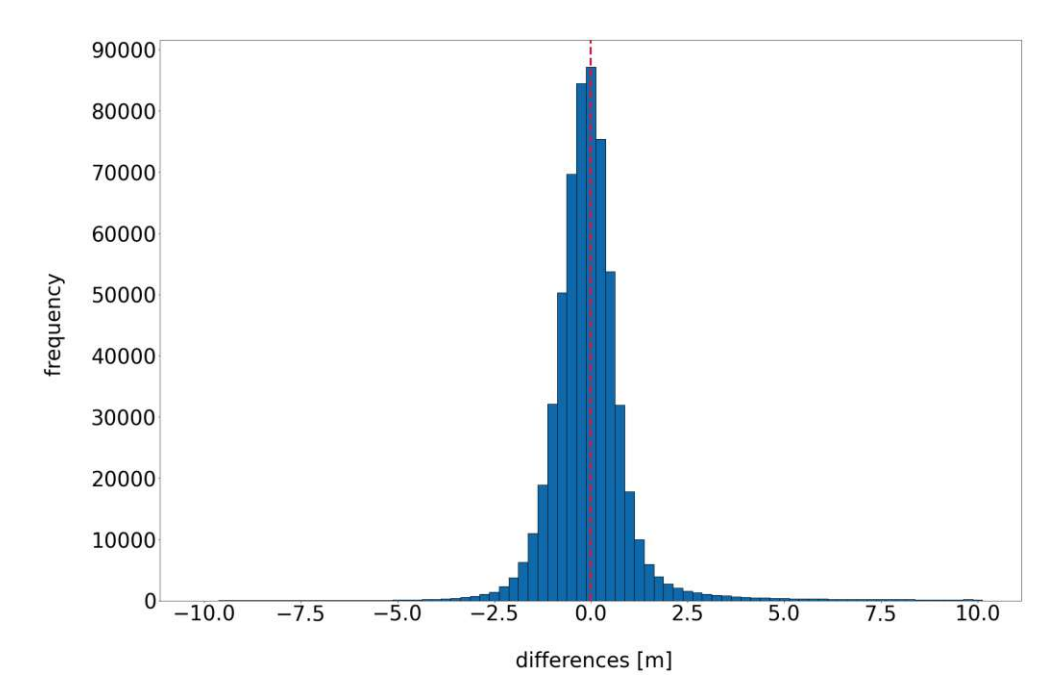
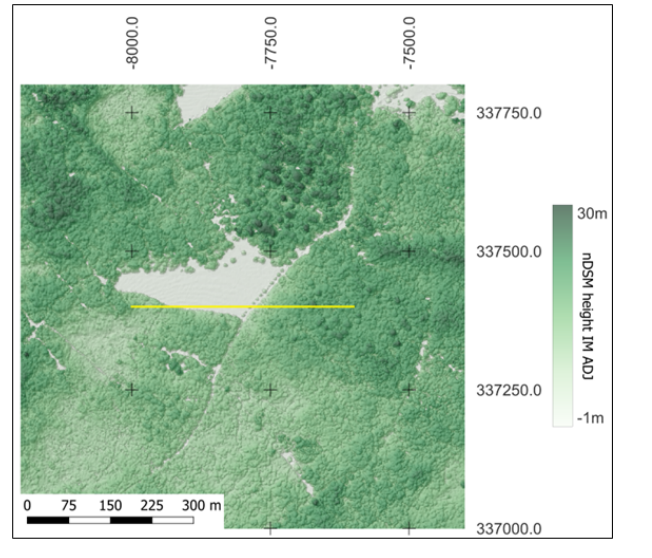


Figure 23: Distribution of the deviations [m] between the adjusted IM model and the reference model on a histogram in the scale range -10 to 10 m with a class width of 0.25 m. The red line indicates a deviation of 0 m from the ground truth within validation area 2.



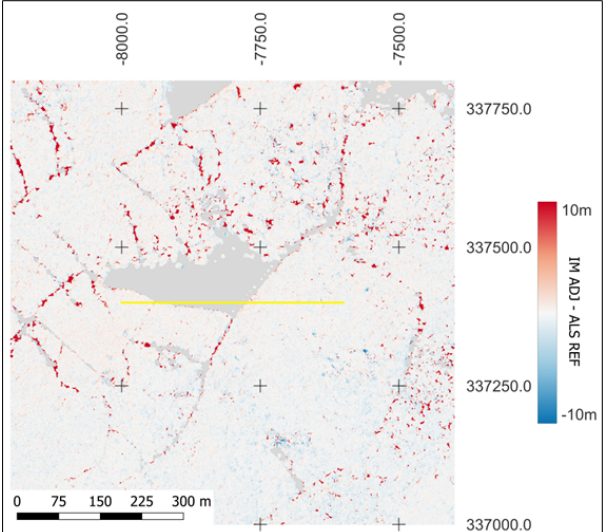


Figure 24: Left: (a) Illustration of the adjusted normalised elevation model in validation area 2, between -1 m (light) and 43 m (dark). Right: (b) Representation of the difference image between the reference ALS and the nDSM adjusted from the IM. In both plots, the yellow line shows the investigation area for the canopy height plot.



Tab. 5: Statistical characteristics of the differences between ground truth and the adjusted IM model in validation area 2. The adjustments compared to the original difference between the given IM CHM and the  $ALS_{REF}$  CHM are shown in the lower part of the table for the values mean, median and RMSE.

Deviation be	${f tween}{f IM}_{AD}$	$_{J}$ & ALS	Deviation	between IM	& ALS
$\overline{\mathbf{Mean}_{ADJ}}$	$\mathbf{Median}_{ADJ}$	$\mathbf{RMSE}_{ADJ}$	$Mean_{REF}$	$Median_{REF}$	$oldsymbol{RMSE}_{REF}$
0.14 m	- 0.09 m	2.07 m	- 0.23 m	- 0.5 m	2.14 m
Adjustments					
+ 0.37 m	+ 0.41 m	- $0.07 \mathrm{m}$			

In the second validation data set, notable improvements and approximations within the adjusted IM CHM (red) to the reference (black) can be recognized in Figure 25, maintaining the overall characteristics of the initial IM data set (blue). The adjusted IM nDSM shows a relatively homogeneous performance across the variance of heights. However, differences occur in non-high vegetated areas, particularly in open spaces, where wave-shaped height differences between the ALS and IM data become apparent.

Furthermore, discrepancies are evident in areas with smaller gaps within the closed canopy, where the IM adjustments deviate from the reference. It is noteworthy that these deviations pose a challenge, highlighting the need for a more robust prediction model in such settings.

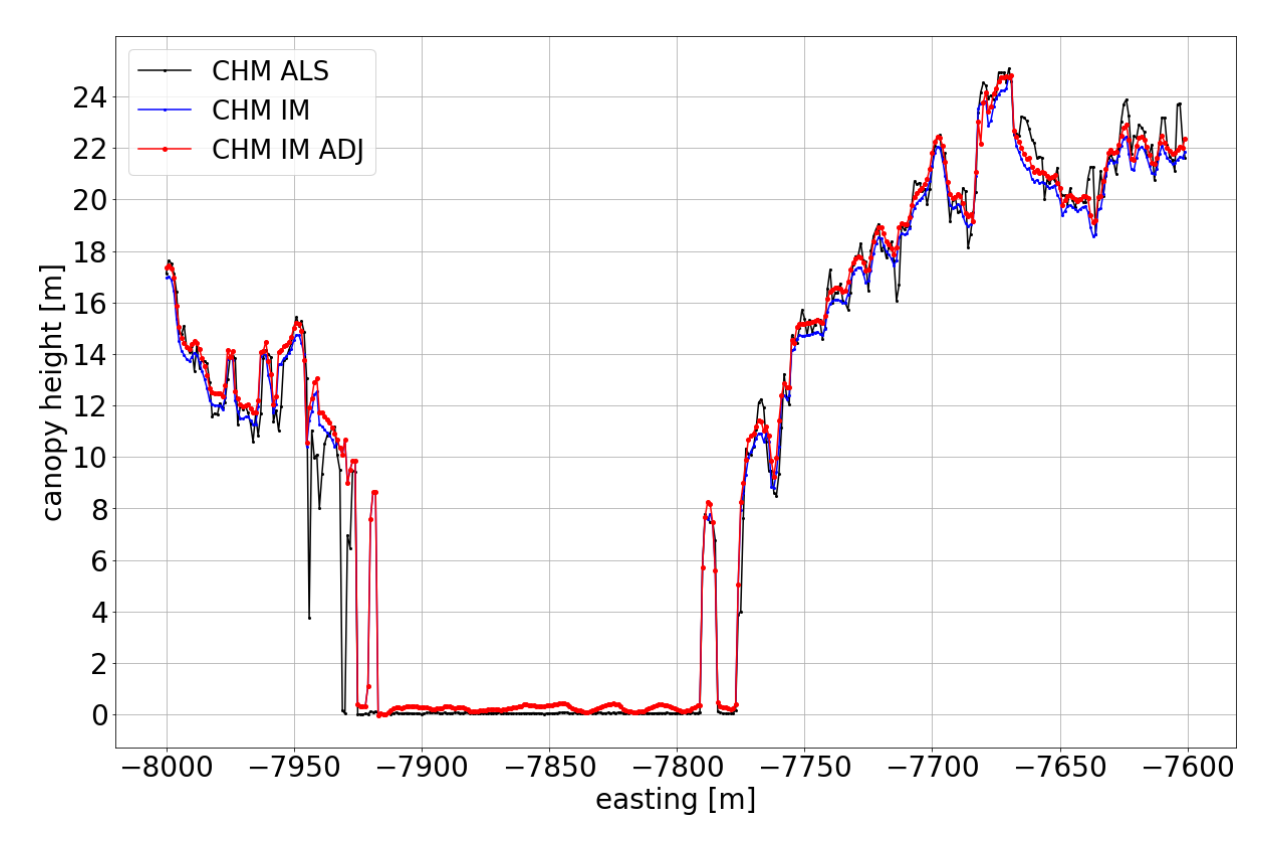


Figure 25: Presentation of the canopy height plot within the selected strip in validation area 2. ALS nDSM heights are shown in black and the input values of the IM nDSM in blue. The adjusted IM values are visualised red in the plot.

### 4.3.3 Validation: Area 3

The height deviations of the adjusted IM model in the third and last validation area are shown in Figure 26. The values are normally distributed around the range between -0.25 m to 0 m deviation, although there are strong over- and underestimations (outliers) as in the histograms in the previous chapters. The median of the data presented in the range of  $\pm$  10 m by using a histogram is -0.16 m, which means that there is an underestimation of the model compared to the reference as in the adjustment before. The largest positive deviation from the given ALS nDSM reaches a value of 45.71 m. The largest underestimation, which represents the minimum of all deviations, is -29.31 m.

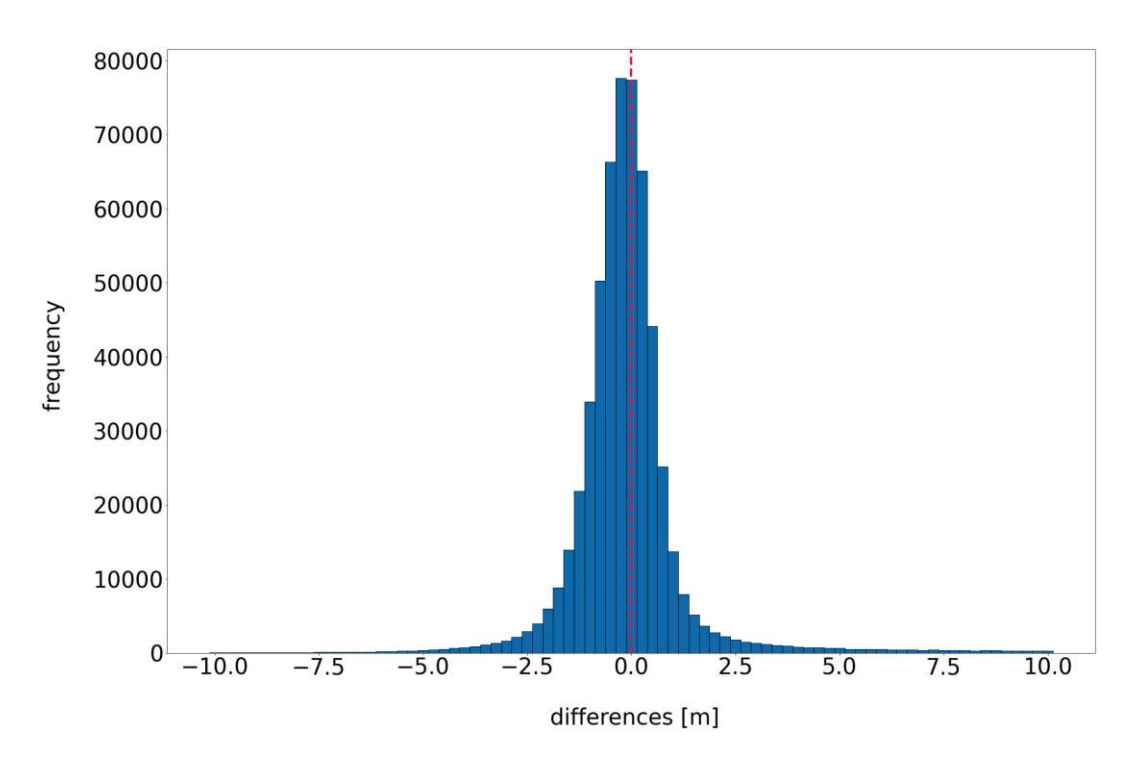
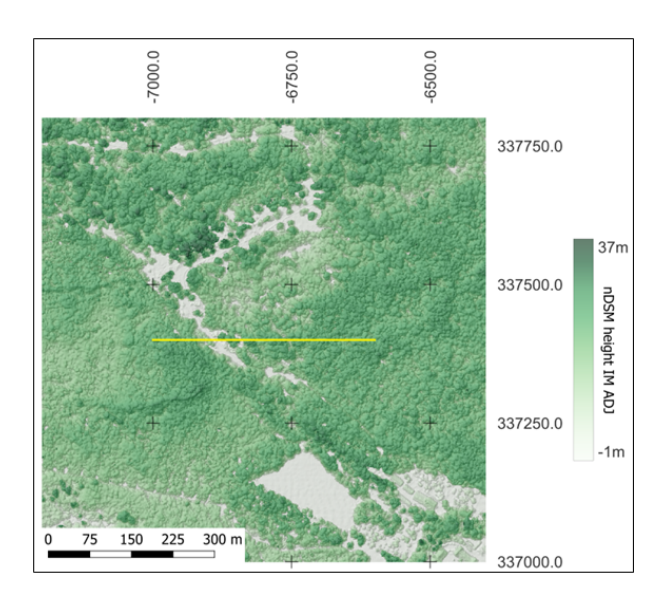


Figure 26: Distribution of the deviations [m] between the adjusted IM model and the reference model on a histogram in the scale range -10 to 10 m with a class width of 0.25 m. The red line indicates a deviation of 0 m from the ground truth within validation area 3.

Figure 27(a) displays the nDSM adjusted from the random forest regression. The values range from -1 m to 37 m, with light green indicating low values and dark green representing high normalised heights. The yellow line indicates the one by 400 pixel wide segment used for the Canopy Height Plot in Figure 28. The difference map for the deviations between the reference CHM and the adjusted IM CHM for the same region is visualised in Figure 27(b). The colour scale ranges from -10 m in blue, representing underestimations, to 0 m deviation in white and extends to overestimations of 10 m in red. Grey areas denote areas outside the canopy mask, where no CHM is available. In all areas with visible gaps and forest aisles from the ALS data set as mentioned in the previous models, the gaps and aisles are displayed too high and are not sufficiently corrected. In the remaining areas of the canopy, the algorithm delivers satisfactory results.



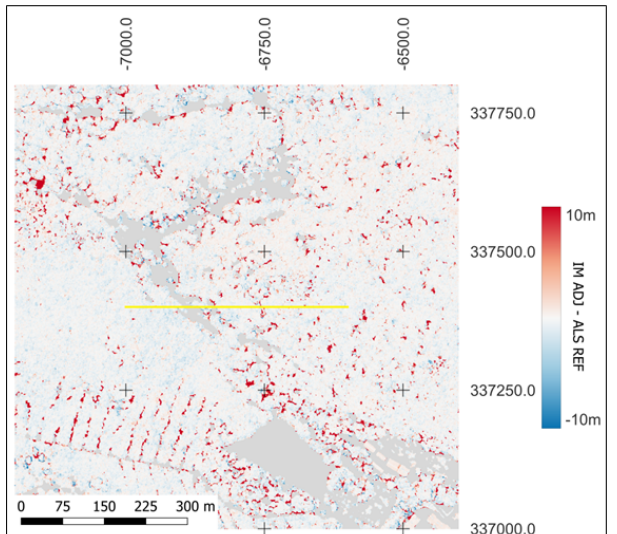


Figure 27: Left: (a) Illustration of the adjusted IM normalised elevation model in validation area 3, between -1 m (light) and 43 m (dark). Right: (b) Representation of the difference image between the reference ALS and the adjusted IM nDSM. In both plots, the yellow line shows the investigation area for the canopy height plot.

The statistical parameters of the third validation area show a mean value of 0.2 m for the height deviations between the adjusted and the reference model. This marks a notable shift of the mean value of 0.27 m from a negative to a positive value compared to the previous mean deviation of -0.07 m. The median was -0.51 m before using the random forest regression and an improvement by 0.35 m to a median of -0.16 m using the trained model could be achieved. This corresponds to an refinement of around 68%. Similarly, the RMSE of the deviations could be reduced by 0.12 m reaching a value of 2.8 m after applying the random forest regression.

Tab. 6: Statistical characteristics of the differences between ground truth and the adjusted IM model in validation area 1. The adjustments compared to the original difference between the given IM CHM and the  $ALS_{REF}$  CHM are shown in the lower part of the table for the values mean, median and RMSE.

Deviation be	${f etween~IM}_{AD.}$	$_{J}$ & ALS	Deviation	between IM	& ALS
$\overline{\mathbf{Mean}_{ADJ}}$	$\mathbf{Median}_{ADJ}$	$\mathbf{RMSE}_{ADJ}$	$Mean_{REF}$	$Median_{REF}$	$\pmb{RMSE}_{REF}$
0.20 m	-0.16 m	2.80 m	-0.07 m	$-0.51 \ m$	2.92 m
${f Adjust ments}$					
+ 0.27 m	+ 0.35 m	- 0.12 m			_

The canopy height plot confirms the previously presented statements. While the IM model is adapted to the given  $ALS_{REF}$  model, the characteristic properties of the IM persist, resulting in a smoother canopy than expected by the ground truth ALS. This implies that small-scale height differences are not sufficiently modelled from the IM dataset. Gaps that are large enough to be present in the original IM dataset and therefore have a canopy coverage of less than 90% are directly transferred into the adjusted model. In areas with gaps in the  $ALS_{REF}$  dataset but without gaps in the IM nDSM, the prediction fails to undergo sufficient adjustment.

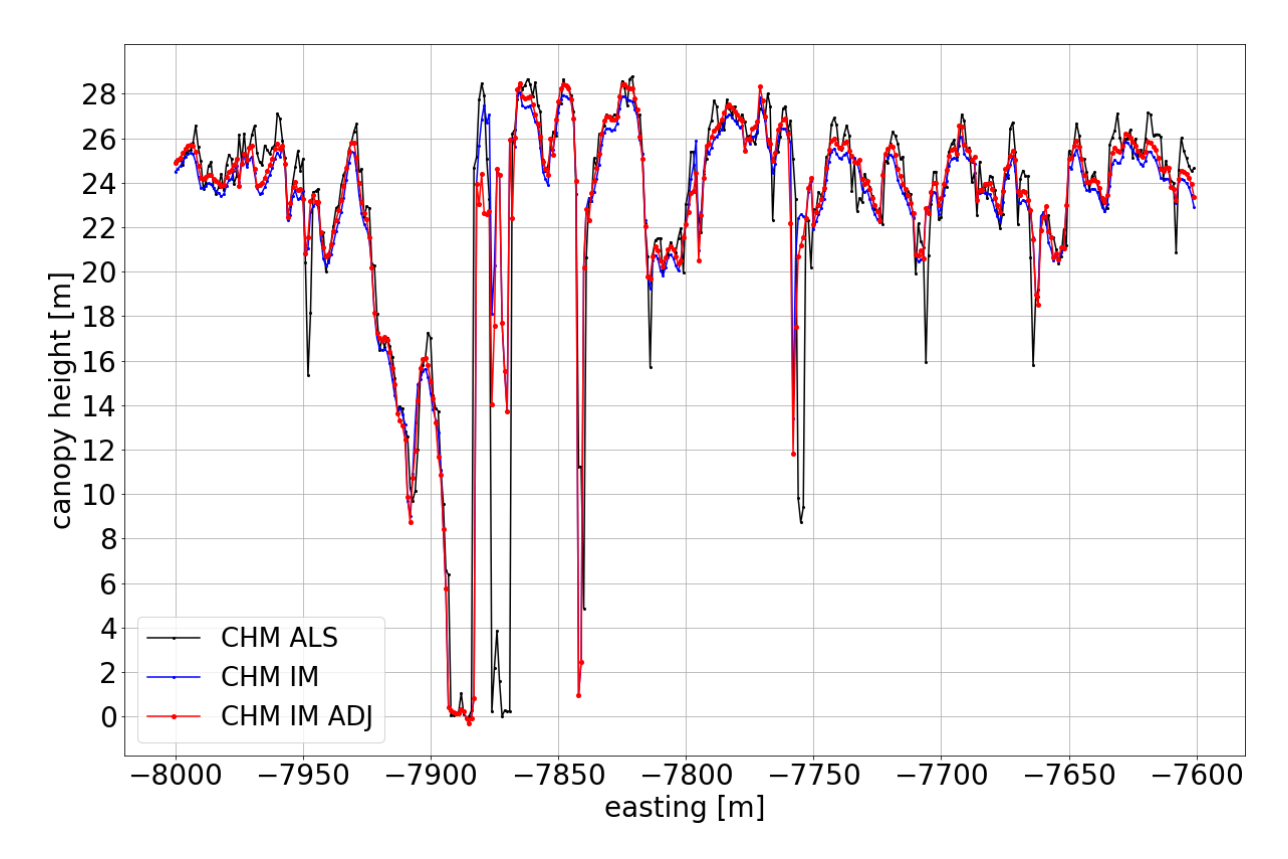


Figure 28: Presentation of the canopy height plot within the selected strip in validation area 3. ALS nDSM heights are shown in black and the input values of the IM nDSM in blue. The adjusted IM values are shown as red in the plot.

To enhance the precision of the statements presented in the previous chapters, the medians before and after the adjustment of the random forest regression were visualised in Figure 29. For this purpose, the values within the IM nDSM were divided into classes of 2 m, and the medians of the height deviations between IM and ALS were calculated both before and after the regression model. Since the height classes, scaled between 0 m and 40 m, also include non-removed outliers, the outlier-resistant median was used for this analysis.

It is important to consider the scaling of the three histograms in Figure 29. Outliers above the defined threshold of 40 m, as well as incorrectly adjusted values below the DTM in the  $IM_{ADJ}$ , resulting in a negative CHM height class, were excluded from this graph to avoid complicating the visualisation. It should also be noted that values in the histogram



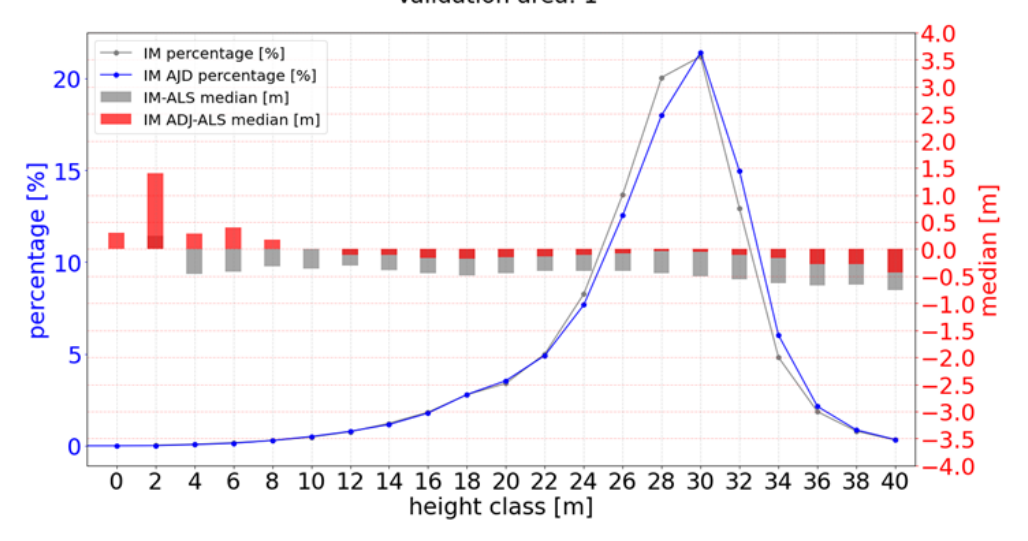
converging towards zero do not assume the value zero, rather they represent only a small percentage of the population.

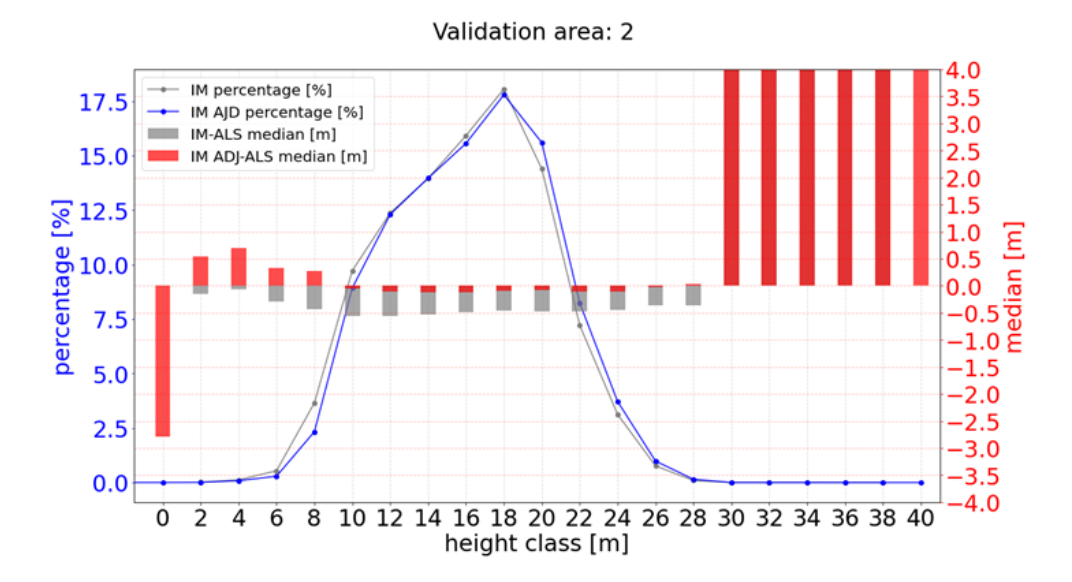
In Figure 29, one can observe that there are no significant outliers in the height classes containing many pixels of the CHM, indicating an improvement in the deviations. In the first validation area, in particular, deviations of more than 4 m are not present.

In the second validation area, it is observed that in the height class around 40 m, values only fall into this class after the adjustment has been applied. Due to their relatively low occurrence within the total mass, outliers from the class of 30 m only have a minor influence. Similarly, validation area three shows a clear, though numerically low, deviation for height values within the canopy mask for values below 2 m.

In summary, in all three validation areas, an improvement in the median of the deviations between the IM and the ALS could be achieved by applying the random forest regression.

### Validation area: 1





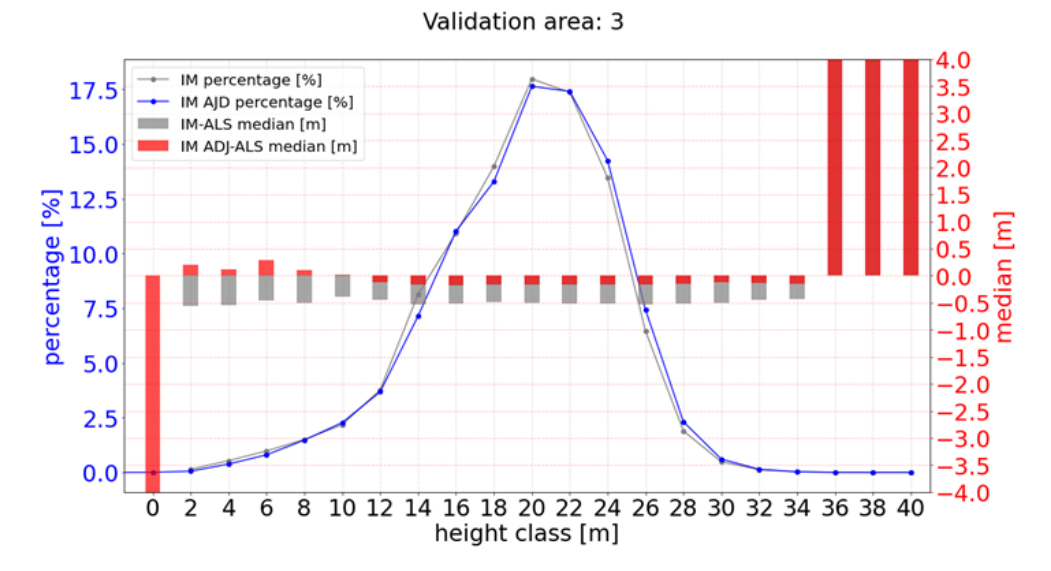


Figure 29: Percentage (line) and median (bar) of height differences between the IM and  $ALS_{REF}$ nDSM before and after applying the random forest regression.



## 5 Discussion

The main objective of this study was to assess the feasibility of aligning data acquired through image matching of aerial images with data gathered from the state-of-the-art airborne laser scanning flight campaigns (Honkavaara et al., 2013). To move away from a computationally intensive point-based approach raster images of these, point clouds were generated. Digital surface models and especially canopy height models out of ALS (Mielcarek et al., 2018) or aerial images are often used in forest applications (Lisein et al., 2013). For this study, high-resolution raster images of 1 by 1 metre were generated for the derivation of the surface heights. These DSMs were then normalised by using a Digital Terrain Model of the City of Vienna and served as the main input data for further computation.

When looking at a difference image, the generated topographic models tend to show an underestimation of the height by the image matching method compared to the results of airborne laser scanning within the closed canopy. In areas with smaller openings within this closed canopy structure, significant deviations between the image matching method and the detection of the actual situation captured by ALS can be observed. Outside the closed area, the two derived height models are practically identical after the transformation of both models into the same height system. In general, the models derived from the IM method provide a comparatively smoother surface and were able to penetrate less deeply in smaller openings than the model from the ALS flights, which were more accurate in representing the individual small-scale characteristics (Luethje et al., 2017; Honkavaara et al., 2013).

To be able to reduce the non-systematic deviations between the two recording methods as effectively as possible, a random forest regression was trained. To train the regression,

a difference matrix with the individual height differences was calculated from the previously created nDSMs. Corresponding to each difference value within this matrix, several statistical parameters were then added at the corresponding position. These parameters were calculated from the moving window algorithm using the IM nDSM. For this purpose, classic and easy-to-implement parameters such as quantiles, range and standard deviation of the height values were calculated for the raster image.

During the training process, it became apparent that a smaller neighbourhood around the pixel in the calculation of these statistical parameters produced better results than tests which included a relatively large neighbourhood. Furthermore, better results for the prediction accuracy were achieved with models that have a lower maximum depth in random forest training. Similarly, the results indicate that an increase in the number of estimators does not show direct improvements. An optimal enhancement was demonstrated by minimising the RMSE, as this is the most common metric for measuring the accuracy of regression analyses (Dewi & Chen, 2019). This minimal RMSE could be achieved through the usage of a small kernel size of 1 in the training and a maximum depth set at ten, along with 30 estimators.

The results within the test and validation areas show an improvement in the height deviations between ALS and IM. Compared to the original deviation in the validation area, the median of the height differences over the entire canopy of all three validation regions was improved by an average of 77%. The improvement of the RMSE, which is more sensitive to outliers due to their weighting, was improved by 3.8% compared to the original deviation between IM and ALS after applying the random forest regression. This smaller improvement can mainly be explained through the large divergence between the adjusted IM and the ALS model assumed to be ground truth. These large deviations, especially in smaller openings within the canopy such as forest aisles, could not be adequately corrected

and are therefore reflected in both the RMSE and the mean value of the deviation between the two models.

As already described by Hobi and Ginzler (2015), especially forests and trees are the most difficult surface elevation models to visualise in relation to different surface covers. The histograms depicting height differences between IM and  $ALS_{REF}$  reveal a persistent underestimation of canopy heights, even after the application of the random forest regression. This observation also matches the research of Hobi and Ginzler (2015), as they also an underestimation of the IM data compared to their reference values in relation to a negative median when applying a cell size of 0.5 m on their dataset.

### Limitations

The application of a random forest regression to minimise non-systematic height deviations between two sampling methods using their nDSMs delivers successful results. As previously described, an improvement in these height differences was achieved within the AOI, located in Wienerwald biosphere reserve.

However, challenges arise particularly in this region due to thinning and forest aisles. Because of the matching process of the given IM data, these special parts of the forest are not detected and therefore cannot be displayed correctly. An approach to recognise these anomalies within the closed canopy cover was attempted using statistical parameters. All statistical parameters which were implemented in OPALS were used for this purpose. However, these models were not adept enough to discern deviations in vegetation or distinguish them from the closed canopy.

In this study, the elimination of outliers was only applied to the ALS point cloud, while the IM data was previously assumed to be adjusted. The ALS data was cleaned using a calculated 98<sup>th</sup> quantile grid based on the Z-values. When deleting outliers, only those which exceeded a threshold of 2 m were considered. Those with a negative value have not been cleaned due to this approach. For further research, also those points which are far too low need to be considered even though, a more detailed look at the negative outliers revealed that most of them were eliminated by applying the canopy mask. The majority of those pixels within the calculated nDSMs lie outside the mask, especially around Grünauer Teich and therefore have a fractional cover of under 90%. To improve the results as well as the training in general such points need to be eliminated in future research.

The visualisation and improvement of strongly divergent edges, meaning the transitions between forest and non-forest areas, is of particular interest. These are represented smoother in the IM dataset than they are in reality and therefore require further correction than the areas of closed forest. Nevertheless, training the dataset is exceptionally challenging due to the lack of geographical overlap in forest boundaries between ALS and IM, particularly in the canopy. It would also not be beneficial to include these non-overlapping areas in the random forest regression, as conducted in this study. As the presence of these highly divergent edge areas would distort the entire regression model.

One of the main limitations of the trained random forest regression relates to the data used. The type of forest in particular was not analysed in detail. No distinction was made between young and old-growth forest. Similarly, due to the available data, no statements could be made about the extent to which the time of recording and the resulting foliage status play a role. The same applies to the implementation of the test process in relation to different types of vegetation, such as different tree species, generally between deciduous and coniferous forest. This limitation must be taken into account when applying the regression and also when analysing the evaluation.

## 6 Conclusion

In this thesis, a method for reducing the non-systematically height differences between normalised airborne laser scanning surface models and those generated from (pixel-based) image matching methods was developed. A self-developed python script applying scikitlearn's random forest regression was used for predicting height adjustment parameters on a pixel-based approach. These corrections were derived from both the IM nDSM as well from its statistical parameters when applying the trained RF model. An area of Wienerwald biosphere reserve was defined as the AOI for training as well as testing and applying this algorithm. The evaluation of the new normalised height values of the adjusted surface model, reveals an improvement for pixels within the closed canopy area. However, noticeable changes in prediction accuracies could be observed when looking at forest aisles within the closed canopy area. The trained regression model provides less reliable results for areas with high height differences (gaps) compared to regions with homogeneous surfaces.

In the process of developing this algorithm, various potential improvements for refining the created program were identified. A prospective improvement for future research entails incorporating distinct masks for different parts of the area to be adjusted. This approach would divide the area into 4 basic parts:

- $\rightarrow$  canopied area
- $\rightarrow$  forest edge
- $\rightarrow$  open areas with low vegetation
- $\rightarrow$  man-made structures such as buildings

The first class can be taken directly from this research and derived from the 90% canopy cover. Forest edges would need to be trained as a buffer around the created canopy mask

to be able to adjust values even if the exact boundary does not overlap. A third option would be to adjust the heights between ALS and IM in relation to open areas not covered with high vegetation. All areas created by humans, such as buildings, should be excluded to avoid the risk of training being falsified using the cadastral map (available as a digital cadastral map in all federal states).

To increase the prediction accuracy for gaps within the canopy, other non-statistical parameters may be considered such as the openness angle of each pixel. The openness of a pixel (see OPALS, n.d.-b; Yokoyama et al., 2002) describes the opening angle for a cone for each pixel in a 3D raster image. This additional value could make it possible to describe such areas that are not sufficiently visualised in IM by changes in the opening angle.

To improve the algorithm, it should also be considered that a larger-scale approach could be used. The small cell sizes likely play a role in the accuracy and applicability of the regression model. Improvements are not always achieved within the algorithm. For some height levels, unfortunately, the deviation also deteriorates. With a larger cell size, smaller-scale height differences would play a smaller role.

To prevent an adjustment that worsens the model, only values that do not exceed a certain threshold of adjustment to the reference model should be considered in future. In this way, possible outliers caused by the application of the random forest model within the canopy can be avoided.

What also needs to be considered when applying this regression, is that the foliage status might also be significant for the prediction and adjustment for the models derived. An increased understanding of the performance for different forest types but also topographic conditions would be necessary to assess the applicability of the trained regression model

TU **Bibliothek**, Die approbierte gedruckte Originalversion dieser Diplomarbeit ist an der TU Wien Bibliothek verfügbar wien knowledge hub. The approved original version of this thesis is available in print at TU Wien Bibliothek.

to other regions. In future research, not only different forest areas should be tested in terms of their vegetation, but also data from different seasons should be investigated. By adding additional data from different years as well as different seasons, it may also be possible to draw conclusions as to whether corrections are needed for specific forest types, such as the difference between young and old forests or between deciduous and coniferous trees, as these have different characteristics in terms of growth behaviour and data recording.

In conclusion, this method offers a reliable way to cleaning data obtained from image matching procedures in aerial imagery. This holds especially true for areas that are not actively cultivated for forestry, such as nature reserves or, as in this case, the Johannser Kogel core zone. The capability to compare annual data from aerial images with stateof-the-art ALS offers the possibility for close-meshed temporal monitoring of forests and individual trees. In addition, reference values from ALS can be complemented with temporally high-resolution IM data for biomass determination and the assessment of forest and canopy areas

## 7 References

Aufreiter, C., & Schöttl, S. (2019). The influence of outliers in image matching point clouds on canopy height models and growing stock estimations. [Internal document: Bundesforschungszentrum für Wald (BFW)]

Ali-Sisto, D., & Packalen, P. (2017). Forest Change Detection by Using Point Clouds From Dense Image Matching Together With a LiDAR-Derived Terrain Model. IEEE Journal of Selected Topics in Applied Earth Observations and Remote Sensing, 10, 1197–1206. doi:10.1109/JSTARS.2016.2615099

Balogun, A.-L., & Tella, A. (2022). Modelling and investigating the impacts of climatic variables on ozone concentration in Malaysia using correlation analysis with random forest, decision tree regression, linear regression, and support vector regression. Chemosphere, 299, 134250. doi:10.1016/j.chemosphere.2022.134250

Beheshti, N. (2022). Random Forest Regression, A basic explanation and use case in 7 minutes. Towards Data Science. Retrieved from https://towardsdatascience.com/ random-forest-regression-5f605132d19d Last accessed 03.11.2023

Biosphärenpark Wienerwald Management GmbH. (2020). Biosphärenpark Wienerwald, ein Biosphärenpark am Rande einer Millionenstadt. Retrieved from https://www.bpww.at/ sites/default/files/download\_files/BPWW\_Imagefolder\_170x210\_Internet.pdf Last accessed 13.11.2023



Biosphärenpark Wienerwald Management GmbH. (n.d.). Kernzone Johannser Kogel. Retrieved from https://www.bpww.at/sites/default/files/download\_files/ KZO\_Johannser\_Kogel\_screen.pdf Last accessed 13.11.2023

Bruggisser, M. M., Dorigo, W., Dostálová, A., Hollaus, M., Navacchi, C., Schlaffer, S., & Pfeifer, N. (2021). Potential of Sentinel-1 C-Band Time Series to Derive Structural Parameters of Temperate Deciduous Forests. Remote Sensing, 13(4), 1–30.

doi:10.3390/rs13040798

Bundesamt für Eich und Vermessungswesen (BEV). (2019). Remote Sensing - Brochure (English). Retrieved from https://www.bev.gv.at/Services/Produkte/Digitales-Oberflaechenmodell/Digitales-Oberflaechenmodell.html Last accessed: 20.11.2023.

Bundesamt für Eich- und Vermessungswesen (BEV). (n.d.-a). Höhenreferenzsysteme. Retrieved from https://transformator.bev.gv.at/at.gv.bev.transformator/wiki/ lib/exe/fetch.php?media=wiki:hoehenreferenzsysteme\_-\_2020-05-26\_-\_final.pdf Last accessed 17.11.2023

Bundesamt für Eich- und Vermessungswesen (BEV). (n.d.-b). Höhen-Grid plus Geoid -Schnittstellenbeschreibung - Version 1.0.1. Retrieved from https://www.bev.gv.at/ Services/Produkte/Grundlagenvermessung/Hoehen-Grid-plus-Geoid.html Last accessed: 05.11.2023

Bundesministerium für europäische und internationale Angelegenheiten (BMEIA). (n.d.). Sustainable Development Goals (SDG). Retrieved from https://www.bmeia.gv.at/ ministerium/aktuelles/sustainable-development-goals-sdg Last accessed 17.11.2023

Bundesministerium Land- und Forstwirtschaft, Regionen und Wasserwirtschaft (BML) (n.d.). Waldinventur des BFW. Retrieved from https://info.bml.gv.at/themen/wald/ wald-in-oesterreich/wald-und-zahlen/waldinventur2019.html Last accessed: 02.11.2023

Bundesforschungszentrum für Wald (BFW) (2022). Österreichische Waldinventur Waldinformationen aus erster Hand. Umfassend. Kompetent. Aktuell. Retrieved from https://waldinventur.at/#/ Last accessed: 17.11.2023

Bundesforschungszentrum für Wald (BFW) (n.d.). Österreichische Waldinventur Waldinformationen aus erster Hand. Umfassend. Kompetent. Aktuell. Retrieved from https://www.bfw.gv.at/fachinstitute/waldinventur/ Last accessed: 17.11.2023

Casas, Á., García, M., Siegel, R. B., Koltunov, A., Ramírez, C., & Ustin, S. (2016). Burned forest characterization at single-tree level with airborne laser scanning for assessing wildlife habitat. Remote Sensing of Environment, 175, 231–241. doi:10.1016/ j.rse.2015.12.044

Ceccherini, G., Girardello, M., Beck, P. S. A., Migliavacca, M., Duveiller, G., Dubois, G., ... Cescatti, A. (2023). Spaceborne LiDAR reveals the effectiveness of European Protected Areas in conserving forest height and vertical structure. Communications Earth & Environment, 4. doi:10.1038/s43247-023-00758-w

Dewi, C., & Chen, R.-C. (2019). Random forest and support vector machine on features selection for regression analysis. International Journal of Innovative Computing, Information & Control: IJICIC, 15(6), 2027–2037. doi:10.24507/ijicic.15.06.2027

Eysn, L., Hollaus, M., Mücke, W., Vetter, M., & Pfeifer, N. (2010). Waldlückenerfassung aus ALS Daten mittels  $\alpha$ -Shapes. In Publikationen der Deutschen Gesellschaft für Photogrammetrie, Fernerkundung und Geoinformation e.V. (pp. 552–560). Retrieved from http://hdl.handle.net/20.500.12708/42588 Last accessed: 16.11.2023

Ginzler, C., & Hobi, M. L. (2015). Countrywide Stereo-Image Matching for Updating Digital Surface Models in the Framework of the Swiss National Forest Inventory. Remote Sensing, 7(4), 4343-4370. doi:10.3390/rs70404343

Goodbody, T. R. H., White, J. C., Coops, N. C., & LeBoeuf, A. (2021). Benchmarking acquisition parameters for digital aerial photogrammetric data for forest inventory applications: Impacts of image overlap and resolution. Remote Sensing of Environment, 265, 112677. doi:10.1016/j.rse.2021.112677

Hagen-Zanker, A. (2016). A computational framework for generalized moving windows and its application to landscape pattern analysis. International Journal of Applied Earth Observation and Geoinformation, 44, 205-216. doi:10.1016/j.jag.2015.09.010

Hauk, E., Niese, G., & Schadauer, K. (2020). Instruktion für die Feldarbeit der österreichischen Waldinventur. Retrieved from https://bfw.ac.at/700/pdf/DA\_2016\_Endfassung \_klein.pdf Last accessed 10.11.2023

Hollaus, M., Mandlburger, G., Pfeifer, N., & Mücke, W. (2010). Land cover dependent derivation of digital surface models from airborne laser scanning data. Retrieved from https://publik.tuwien.ac.at/files/PubDat\_187839.pdf Last Accessed 17.11.2023

Hollaus, M., Mücke, W., Roncat, A., Pfeifer, N., & Briese, C. (2014). Full-Waveform Airborne Laser Scanning Systems and Their Possibilities in Forest Applications. In: Maltamo, M., Næsset, E., Vauhkonen, J. (Eds.), Forestry Applications of Airborne Laser Scanning (Managing Forest Ecosystems, Vol. 27). Springer, Dordrecht. doi:10.1007/978 -94-017-8663-8\_3

Honkavaara, E., Litkey, P., & Nurminen, K. (2013). Automatic Storm Damage Detection in Forests Using High-Altitude Photogrammetric Imagery. Remote Sensing, 5(3), 1405-1424. doi.org/10.3390/rs5031405

Iglseder, A., Immitzer, M., Dostálová, A., Kasper, A., Pfeifer, N., Bauerhansl, C., ... Hollaus, M. (2023). The potential of combining satellite and airborne remote sensing data for habitat classification and monitoring in forest landscapes. International Journal of Applied Earth Observation and Geoinformation, 117. doi:10.1016/j.jag.2022.103131

Koehrsen, W. (2018). Hyperparameter Tuning the Random Forest in Python. Towards Data Science, Retrieved from https://towardsdatascience.com/hyperparameter-tuning -the-random-forest-in-python-using-scikit-learn-28d2aa77dd74 Last accessed: 20.10.2023

Liu, D., Fan, Z., Fu, Q., Li, M., Faiz, M. A., Ali, S., ... Khan, M. I. (2020). Random forest regression evaluation model of regional flood disaster resilience based on the whale optimization algorithm. Journal of Cleaner Production, 250. doi:10.1016/j.jclepro.2019. 119468



Liu, H., & Dong, P. (2014). A new method for generating canopy height models from discrete-return LiDAR point clouds. Remote Sensing Letters, 5, 575–582. doi:10.1080/ 2150704X.2014.938180

Luethje, F., Tiede, D., & Eisank, C. (2017). Terrain Extraction in Built-Up Areas from Satellite Stereo-Imagery-Derived Surface Models: A Stratified Object-Based Approach. IS-PRS International Journal of Geo-Information, 6, 9. doi:10.3390/ijgi6010009

Lund, G. (2016). National Definitions of Forest/Forestland Listed by Country. Retrieved from https://www.researchgate.net/publication/305776337\_National\_Definitions 

Lisein, J., Pierrot-Deseilligny, M., Bonnet, S., & Lejeune, P. (2013). A photogrammetric workflow for the creation of a forest canopy height model from small unmanned aerial system imagery. Forests, 4(4), 922-944. doi:10.3390/f4040922

Mandlburger, G., Lehner, H., & Pfeifer, N. (2019). A comparison of single photon and full waveform lidar. ISPRS Ann. Photogramm. Remote Sens. Spatial Inf. Sci., IV-2/W5, 397-404. doi:10.5194/isprs-annals-IV-2-W5-397-2019

Mielcarek, M., Stereńczak, K., & Khosravipour, A. (2018). Testing and evaluating different LiDAR-derived canopy height model generation methods for tree height estimation. International Journal of Applied Earth Observation and Geoinformation, 71, 132-143. doi:10.1016/j.jag.2018.05.002

Morakami, H., Nakagawa, K., Hasegawa, H., Shibata, T., & Iwanami, E. (1999). Change detection of buildings using an airborne laser scanner. ISPRS Journal of Photogrammetry and Remote Sensing, 54, 148-152. doi:10.1016/S0924-2716(99)00006-4

Morsdorf, F., Kötz, B., Meier, E., Itten, K. I., & Allgöwer, B. (2006). Estimation of LAI and fractional cover from small footprint airborne laser scanning data based on gap fraction. Remote Sensing of Environment, 104(1), 50-61. doi:10.1016/j.rse.2006.04.019

Næsset, E., & Gobakken, T. (2005). Estimating forest growth using canopy metrics derived from airborne laser scanner data. Remote Sensing of Environment, 96, 453-465. doi:10.1016/j.rse.2005.04.001

National Oceanic and Atmospheric Administration Coastal Services Center (NOAA) (2012). Lidar 101: An Introduction to Lidar Technology, Data, and Applications. Retrieved from https://coast.noaa.gov/data/digitalcoast/pdf/lidar-101.pdf Last accessed: 25.10.2023

Navarro, J. A., Fernández-Landa, A., Tomé, J. L., Guillén-Climent, M. L., & Ojeda, J. C. (2018). Testing the quality of forest variable estimation using dense image matching: a comparison with airborne laser scanning in a Mediterranean pine forest. International Journal of Remote Sensing, 39, 4744–4760. doi:10.1080/01431161.2018.1471551

OPALS (2016-a). Module DSM. Retrieved from https://opals.geo.tuwien.ac.at/html/ stable/ModuleDSM.html Last accessed 11.11.2023

OPALS (2016-b). ModuleStatFilter. Retrieved from https://opals.geo.tuwien.ac.at/ html/stable/ModuleStatFilter.html Last accessed 11.11.2023

OPALS (n.d.-a). for Tree Detection. Retrieved from https://opals.geo.tuwien.ac.at/ html/stable/forTreeDetection.html Last accessed 11.11.2023

OPALS (n.d.-b). *Module Openness*. Retrieved from https://opals.geo.tuwien.ac.at/ html/stable/ModuleOpenness.html Last accessed 11.11.2023

Österreichische Bundesforste (ÖBf). (2023). Digitale Waldinventur: Forschungsinitiative testet Einsatz von künstlicher Intelligenz im Bundesforste-Wald. Retrieved from https://www.bundesforste.at/service-presse/presse/pressedetail/news/digitale -waldinventur-forschungsinitiative-testet-einsatz-von-kuenstlicherintelligenz-im-bundesforste-wald.html Last accessed 19.11.2023

Pfeifer, N., Mandlburger, G., Otepka, J., & Karel, W. (2014). OPALS - A framework for Airborne Laser Scanning data analysis. Computers, Environment and Urban Systems, 45, 125-136. doi:10.1016/j.compenvurbsys.2013.11.002

Pfeifer, N., Rutzinger, M., Rottensteiner, F., Muecke, W., & Hollaus, M. (2007). Extraction of building footprints from airborne laser scanning: Comparison and validation techniques. Urban Remote Sensing Joint Event, Paris, France, 2007, 1-9. doi: 10.1109/URS.2007.371854

Puliti, S., Dash, J. P., Watt, M. S., Breidenbach, J., & Pearse, G. D. (2020). A comparison of UAV laser scanning, photogrammetry, and airborne laser scanning for precision inventory of small-forest properties. Forestry: An International Journal of Forest Research, 93(1), 150-162. doi:10.1093/forestry/cpz057

Puliti, S., Solberg, S., & Granhus, A. (2019). Use of UAV Photogrammetric Data for Estimation of Biophysical Properties in Forest Stands Under Regeneration. Remote Sensing, 11, 233. doi:10.3390/rs11030233

Ranacher, L., Lapin, K., & Hesser, F. (2023). Biodiversität und die Nutzung des Waldes. In: Hesser, F., Braun, M. (Hrsg.), Waldbewirtschaftung in der Klimakrise. Studien zum Marketing natürlicher Ressourcen. Springer Gabler, Wiesbaden. doi:10.1007/978-3 -658-39054-9\_7

Rao, B. S., Kumar, G. A., Runjhun, C., Rao, C. V. K. V. P. J., & Babu, G. V. (2022). Improvement of Airborne LiDAR Intensity Image Content with Shaded nDSM and Assessment of Its Utility in Geospatial Data Generation. Journal of the Indian Society of Remote Sensing, 50, 507-521. doi:10.1007/s12524-021-01468-6

Rastiveis, H., Khodaverdi Zahraee, N., & Jouybari, A. (2018). Object-oriented classification of LiDAR data for post-earthquake damage detection. International Archives of the Photogrammetry, Remote Sensing and Spatial Information Sciences, XLII-3/W4, 421-427. doi:10.5194/isprs-archives-XLII-3-W4-421-2018

Ressl, C., Brockmann, H., Mandlburger, G., & Pfeifer, N. (2016). Dense Image Matching vs. Airborne Laser Scanning – Comparison of two methods for deriving terrain models. Photogrammetrie - Fernerkundung - Geoinformation, 2016, Heft 2, 57–73. doi:10.1127/ pfg/2016/0288

scikit-learn. (n.d.). RandomForestRegressor. Retrieved from https://scikit-learn. org/stable/modules/generated/sklearn.ensemble.RandomForestRegressor.html Last accessed: 01.11.2023

Stadt Wien - Stadtvermessung (n.d.). Stadtplan Orthofoto. Retreived from https://www.wien.gv.at/stadtentwicklung/stadtvermessung/geodaten/orthofoto/ stadtplansuche.html Last accessed: 04.11.2023

Tran, T., Ressl, C., & Pfeifer, N. (2018). Integrated Change Detection and Classification in Urban Areas Based on Airborne Laser Scanning Point Clouds. Sensors, 18, 448. doi:10.3390/s18020448

Umweltbundesamt. (n.d.). Natura 2000. Retrieved from https://www.umweltbundesamt .at/umweltthemen/naturschutz/schutzgebiete/natura2000 Last accessed: 02.11.2023

United Nations - Department of Economic and Social Affairs. (2023). SDG indicator metadata - Harmonized metadata template. Retrieved from https://unstats.un.org/ sdgs/metadata/files/Metadata-15-01-01.pdf Last Accessed 17.11.2023

United Nations Educational Scientific and Cultural Organization (UNESCO). (2021). Biosphere Reserves. Retrieved from https://en.unesco.org/biosphere Last accessed: 02.11.2023.

Ullah, S., Adler, P., Dees, M., Datta, P., Weinacker, H., & Koch, B. (2017). Comparing image-based point clouds and airborne laser scanning data for estimating forest heights. iForest - Biogeosciences and Forestry, 10, 273-280. doi:10.3832/ifor2077-009

Vereinte Nationen - Regionales Informationszentrum der Vereinten Nationen (UNRIC) (2019). UN-Mitgliedstaaten. Retrieved from: https://unric.org/de/mitgliedstaaten/ Last accessed: 17.11.2023

Viana-Soto, A., García, M., Aguado, I., & Salas, J. (2022). Assessing post-fire forest structure recovery by combining LiDAR data and Landsat time series in Mediterranean pine forests. International Journal of Applied Earth Observation and Geoinformation, 108. doi:10.1016/j.jag.2022.102754

Venkateswarlu, D. (2013). Definition of Forests: A Review. Retrieved from https:// data.opendevelopmentmekong.net/dataset/1937c446-b07f-4fba-a577-1f299da1cced/resource/e70454d6-ff1c-4eeb-b988-ac40cfc5ca3f/download/ venkateswarlu.pdf Last accessed: 17.11.2023

White, J. C., Coops, N. C., Wulder, M. A., Vastaranta, M., Hilker, T., & Tompalski, P. (2016). Remote Sensing Technologies for Enhancing Forest Inventories: A Review. Canadian Journal of Remote Sensing, 42, 619-641. doi:10.1080/07038992.2016.1207484

Yokoyama, R., Shirasawa, M., & Pike, R. J. (2002). Visualizing Topography by Openness: A New Application of Image Processing to Digital Elevation Models. Photogrammetric Engineering and Remote Sensing, 68(3), 257-266.

Yu, X., Hyyppä, J., Kaartinen, H., & Maltamo, M. (2004). Automatic detection of harvested trees and determination of forest growth using airborne laser scanning. Remote Sensing of Environment, 90, 451-462. doi:10.1016/j.rse.2004.02.001

# 8 Appendix

	Pearson's R [%]	84,14	84,21	83,96	83,76	83,81	83,60	83,58	84,12	84,19	84,10	84,12	84,06	84,05	84,05	84,17	84,17	84,17	84,13	84,11	84,08	84,05	84,20	84,20	84,20	84,10	84,10	84,10	84,10
	RMSE [m]	3,560	3,552	3,576	3,595	3,589	3,609	3,611	3,561	3,555	3,563	3,560	3,565	3,566	3,566	3,556	3,557	3,557	3,559	3,561	3,563	3,566	3,556	3,556	3,555	3,559	3,559	3,559	3,558
	Std. deviation [m]	3,546	3,538	3,563	3,583	3,577	3,598	3,600	3,547	3,541	3,550	3,548	3,553	3,554	3,555	3,542	3,544	3,544	3,630	3,549	3,551	3,555	3,542	3,543	3,541	3,546	3,547	3,548	3,546
Test configuration files	Median [m]	-0,222	-0,224	-0,209	-0,204	-0,205	-0,204	-0,206	-0,225	-0,224	-0,219	-0,221	-0,223	-0,224	-0,224	-0,224	-0.225	-0,221	-0,223	-0,226	-0,226	-0,227	-0,224	-0,225	-0,222	-0,225	-0,228	-0,230	-0,229
configur	Mean [m]	0,317	0,314	0,308	0,292	0,293	0,284	0,280	0,315	0,316	0,307	0,296	0,290	0,288	0,288	0,316	0,313	0,308	0,297	0,291	0,289	0,287	0,316	0,312	0,310	0,297	0,290	0,288	0,288
Test	Max depth	ಬ	10	20	30	40	20	None	2	10	20	30	40	50	None	5	10	20	30	40	20	None	2	10	20	30	40	20	None
	Nr. of estimators	10	10	10	10	10	10	10	30	30	30	30	30	30	30	20	20	50	20	50	20	20	100	100	100	100	100	100	100
	Kernel size	2	2	2	2	2	2	2	2	2	2	2	2	2	2	2	2	2	2	2	2	2	2	2	2	2	2	2	2
	CONFIG	0610_1636	0610_1642	0610_1646	0610_1651	0610_1709	0610_1627	0610_1657	0610_1716	0610_1722	0610_1826	0610_1816	0610_1801	0610_1747	0610_1729	0710_1245	0710_1229	0710_1211	0710_1155	0710_1105	0710_0006	0610_2343	0610_2333	0610_2311	0610_2229	0610_2157	0610_2124	0610_2048	0610_1835



imators Max depth
o E
20
30
40
20
None
22
10
20
30
40
20
None
5
10
20
30
40
20
None
2
10
20
30
40
50
None

CONFIG	Kernel size	CONFIG Kernel size Nr. of estimators	Max depth	Mean [m]	Median [m]	Std. deviation [m]	RMSE [m]	Pearson's R [%]
2410_0910	1	50	5	0,310	-0,216	3,508	3,522	84,52
2410_0923	П	50	10	0,302	-0,217	3,496	3,509	84,64
2410_0933	1	20	20	0,296	-0,214	3,502	3,515	84,59
2410_0947	1	20	30	0,284	-0,217	3,507	3,519	84,53
2410_1048	П	20	40	0,279	-0,218	3,512	3,523	84,48
2410_1104	1	20	20	0,277	-0,219	3,513	3,524	84,47
2410_1125	1	20	None	0,280	-0,219	3,510	3,521	84,50
2410_1143	1	100	2	0,310	-0,216	3,508	3,521	84,52
2410_1150	1	100	10	0,302	-0,218	3,497	3,510	84,64
2410_1202	П	100	20	0,297	-0,215	3,502	3,514	84,59
2410_1249	-	100	30	0,285	-0,218	3,505	3,517	84,55
2410_1323	П	100	40	0,279	-0,221	3,508	3,519	84,52
2410_1503	-1	100	50	0,278	-0,221	3,507	3,518	84,53
2410_1538		100	None	0,278	-0,223	3,507	3,518	84,53